PHILOSOPHICAL TRANSACTIONS OF THE ROYAL SOCIETY A MATHEMATICAL, PHYSICAL & ENGINEERING SCIENCES

Large Amplitude Waves in Bounded Media I. Reflexion and Transmission of Large Amplitude Shockless Pulses at an Interface

H. M. Cekirge and E. Varley

Phil. Trans. R. Soc. Lond. A 1973 **273**, 261-313
doi: 10.1098/rsta.1973.0001

LARGE AMPLITUDE WAVES IN BOUNDED MEDIA I. REFLEXION AND TRANSMISSION OF LARGE AMPLITUDE SHOCKLESS PULSES AT AN INTERFACE

By H. M. Cekirge and E. Varley

Centre for the Application of Mathematics, Lehigh University

(*Communicated by Sir James Lighthill, F.R.S. – Received* 17 *April* 1972)

CONTENTS

Techniques which can be used to analyse the interaction of large amplitude elastic waves in a bounded medium are described. Although presented in the context of uniaxial stretching deformations in an elastic string or bar, these techniques can be used to analyse the behaviour of any system whose response is described by the nonlinear one-dimensional wave equation. In this first paper the bounded medium is contained between two parallel planes which separate it from other similar media. These are of semi-infinite extent along the axis of propagation which is normal to the interfaces.

The paper is in two parts. In the first part the reflexion and transmission of an incident pulse when it arrives at an interface with a semi-infinite medium is described and the ideas of nonlinear impedance, reflexion coefficient and transmission coefficient are introduced. The results are quite general: no special forms for the stress–strain relations of either elastic materials is assumed. The results for a single interface are used to analyse the decay of a pulse as it moves back and forth between two interfaces. This decay

Vol. 273. A. 1234. (Price £1.40; U.S. $3.90) 22 [Published 4 January 1973

occurs because at each contact with the interface energy is radiated across the interface to the surrounding medium. The algorithms obtained have simple graphical interpretations. The general theory is used to discuss the decay of a pulse in a layer of saturated soil which is bounded from above by sea water and from below by rock. This pulse is triggered by a seismic disturbance deep inside the rock. The theory is also used to analyse the decay in the oscillation which occurs in a shock tube when a diaphragm separating air at high pressure from air at atmospheric pressure is ruptured. The bound gas is contained between the closed end of the tube and the contact discontinuity which is generated when the diaphragm bursts.

In the second part of the paper a more detailed account is given of what happens when a pulse is partially reflected and partially transmitted at an interface. This is achieved by noting that the responses of many elastic materials can be correlated, both qualitatively and quantitatively, by a family of stress–strain laws for which the governing nonlinear equations for this problem can be solved exactly. These laws are sufficiently general to locally curve fit any prescribed stress–strain law to an error $O([\text{strain}]^4)$ in some vicinity of the unstrained state. They can also be used to fit the response of a polytropic gas during isentropic flow to within an error of 1 % as the density changes by a factor of ten! The reflexion of a large amplitude pulse from rigid and perfectly free interfaces is given special emphasis as is the reflexion from an interface with a Hookean material.

1. Introduction

Most of the analyses which describe the behaviour of large amplitude waves in elastic materials deal only with progressing waves. The problem of what happens when such waves are reflected from material boundaries has received comparatively little attention. The only significant results which describe the effect of material nonlinearity on waves in bounded media have been obtained in the small amplitude limit when the effect of locally small nonlinearity accumulates to produce a first-order contribution to the disturbance. (A general representation of such small amplitude wave motions was derived in a recent paper by Mortell & Varley (1970).) However, the dynamic responses of many materials are, in fact, grossly nonlinear for the applied tractions to which they are often subjected. For example, foams, some rubbers, soils and clays can harden, or lock, appreciably during uniaxial compression, while collagen tissue and vulcanised rubbers harden in extension. Many polycrystalline solids, on the other hand, soften in compression while gases, which can also be regarded as elastic media, soften in extension. Of course, most of these materials only behave elastically under certain circumstances. Hysteresis effects can play a significant role. Most polycrystalline solids, for example, only behave elastically during compression: during unloading the stress–strain relation differs from particle to particle. Even so, over the times when the material response is essentially elastic, the effect of nonlinear wave interactions can play a dominant role. It is the purpose of this and future papers to describe techniques which can be used to analyse the essential features of some of the more important large amplitude wave interactions which occur in bounded elastic materials. The development of such techniques is necessary before the effect of more complicated material responses on the dynamic behaviours of bounded materials can be analysed.

In this paper we describe some of the main features of the decay of large amplitude disturbances in a slab of elastic material which is contained between two parallel material planes, or interfaces. In the main the deformation is produced by uniaxial stretching waves which propagate in directions normal to the interface. Each interface separates the bounded material from some other elastic material which is also being stretched in the same direction. This surrounding material, which could be air, is of semi-infinite extent in a direction normal to the interface in the sense that, over the time ($t > 0$) the disturbance is analysed, any energy which may be reflected from its other boundaries does not appreciably affect the disturbance in the bounded medium. The disturbance can be thought of as triggered by some known forced motion of one of the interfaces before $t = 0$, or by the wave which is transmitted into the slab when a wave

travelling through one of the surrounding materials is incident at one of the interfaces prior to $t = 0$. An example of the first situation, which is discussed in some detail, occurs when a gas which was contained at a high pressure between the closed end of a shock tube and a diaphragm is set in motion when the diaphragm bursts. The initial discontinuity at the diaphragm splits into two waves: a constant strength shock wave which moves away from the closed end of the tube and a centred expansion wave which moves towards it. It is this expansion wave that triggers the disturbance in the gas which is bounded by the rigid wall and the contact discontinuity, or material plane, which is also generated when the diaphragm bursts. After complete reflexion from the closed end of the tube the expansion wave is partly reflected and partly transmitted at the contact discontinuity. The transmitted wave ultimately catches up with the shock where it too is partially reflected. The analysis presented is only valid for times when this reflected wave has no effect on the gas between the wall and the contact discontinuity. A good example of the second situation, which is also discussed in some detail, occurs in a layer of saturated soil which is bounded by sea water from above and by rock from below when a stretching pulse crosses its interface with the rock. This pulse could be triggered in the rock by a seismic disturbance at a point which is deep compared with the distance between the two interfaces. Then, the pulse is essentially plane as it traverses the saturated soil. The analysis is only valid for times when the energy which is reflected from the interface between the sea and the atmosphere has a negligible effect on the deformation of the saturated soil.

This paper only deals with large amplitude shockless waves. It is in two parts. In the first part we show how to calculate the decay in the amplitude of a pulse as it moves back and forth between free interfaces. During each contact with an interface part of the energy of the pulse is radiated to the surrounding medium. No account of the change in shape of the pulse is given. This rather crude, but sometimes sufficient, information can be obtained without restricting the forms of the equations of state of either the bounded or surrounding elastic media. The results are quite general. In §4.1 we show how to calculate the amplitudes of the reflected and transmitted pulses at an elastic–elastic interface as a function of the amplitude of the incident pulse. This is possible because as long as the transmitted pulse does not develop shocks it is a simple wave. In such a wave the relation between the normal traction and material velocity is determined by the stress–strain relation of the transmitting material. It is independent of the detailed shape of the pulse which is transmitted. Since both traction and normal velocity are continuous at the interface this relation holds on either side of the interface and, in fact, completely determines the reflexion and transmission characteristics of the interface. A discussion of these characteristics is greatly simplified by introducing the ideas of the nonlinear impedance, the nonlinear reflexion coefficient and the nonlinear transmission coefficient of an interface. These quantities occur quite naturally in the analysis and are simple generalizations of those which occur when analysing the reflexion characteristics of an interface separating Hookean materials. For finite amplitude waves, however, these coefficients are functions of the current traction at the interface.

In §4.2 the results established in §4.1 for a single interface are used to calculate the change in the amplitude of a pulse after multiple reflexions from both free boundaries. The amplitudes of the transmitted pulses at each contact with an interface are also calculated. The algorithms derived have a simple graphical interpretation. In §§5 and 6 the general theory is used to provide a detailed account of the decay in the strengths of pulses in a shock tube and in a layer of saturated soil.

The results which are described in the first part of this paper can only be used to calculate the

PHILOSOPHICAL TRANSACTIONS OF THE ROYAL SOCIETY A MATHEMATICAL, PHYSICAL & ENGINEERING SCIENCES

change in strength of a pulse. They cannot be used to calculate its change in shape, or the details of the deformation it produces, as it moves back and forth. It seems a hopeless task to make any really significant headway with this formidable problem without specifying some definite form for the relation between the stress T and the strain e. In practice, for solids this relation is usually determined from experimental data and to the same error that T and e can be measured experimentally this data can be curve fitted by any one of a host of analytic expressions. Usually power laws are tried. Bell (1968), for example, in his extensive study of the dynamic responses of polycrystalline solids during uniaxial compression has shown that the experimental data can be fitted over some range of e by a simple parabolic law. However, even with such a simple stress–strain relation the governing hyperbolic equations cannot be integrated except, of course, when the deformation is generated by a progressing simple wave.

In the second part of this paper we show that the responses of many diverse elastic materials can be correlated, both qualitatively and quantitatively, by the family of stress–strain laws for which T is related to e by equations of the form

$$\frac{\mathrm{d}^2T}{\mathrm{d}e^2} = \bar{\mu}\left(\frac{\mathrm{d}T}{\mathrm{d}e}\right)^{\frac{5}{4}} + \bar{\nu}\left(\frac{\mathrm{d}T}{\mathrm{d}e}\right)^{\frac{7}{4}}, \tag{1.1}$$

where $\bar{\mu}$ and $\bar{\nu}$ are material constants. In §7 it is shown that for this family of *model* equations of state the equations which govern the deformation simplify considerably and many important problems which involve the interaction of large amplitude elastic waves can be solved exactly. In §8 a detailed account of the material responses which can be described by these laws is given. First, in §8.1, it is shown how the parameters $\bar{\mu}$ and $\bar{\nu}$ must be chosen so that the corresponding model stress–strain relation can locally approximate any given stress–strain relation in some vicinity of $(T, e) = (0, 0)$ to within an error of $O(e^4)$. In §8.2 we show that the parameters $(\bar{\mu}, \bar{\nu})$ can also be chosen so that the equation of state of a polytropic gas during isentropic flow can be approximated over a strain range $0 \leqslant e \leqslant 9$ (which corresponds to the density changing by a factor of 10) to within an error which is less than 1 %! The values of the parameters are given when the isentropic exponent $\gamma = \frac{5}{3}$, 1.4 and 1.0. Comparisons between the exact pressure–density relations and the model pressure–density relations are given in tables 1 to 3. In this same section it is shown that Bell's parabolic law can also be approximated by one of the model laws to an error of less than 1 % over the range of strain where Bell's law provides a good fit to the experimental data. The parabolic law and the model law are compared in table 4.

In §§8.3 and 8.4 a detailed description is given of the four main types of material reponses which can be modelled by stress–strain laws which satisfy equation (1.1). These responses are depicted in figures 8 to 11. Figure 8 illustrates the typical response of a soft material, or, more strictly, of a material which softens relative to some reference state where $(T, e) = (0, 0)$. For such a material the sound speed $A[\propto (\mathrm{d}T/\mathrm{d}e)^{\frac{1}{2}}]$ decreases monotonically, from its value A_0 in the reference state, as e either increases or decreases monotonically. However, A never gets below some limiting value $A_\infty < A_0$. The model stress–strain law is completely determined once A_0, A_∞ and some parameter T_I, which measures the rate at which A changes with e, are specified. However, these three parameters can be specified arbitrarily.

When, for all practical purposes, $A_\infty = 0$ a soft material is called ideally soft. Figure 9 illustrates the typical response of such a material. The stress T can only vary in the range $[0, T_\mathrm{I}]$, where the limiting stress T_I is a material constant. The model law is uniquely determined once A_0, T_I and the parameter ϵ, $= e$ when $T = 0.99T_\mathrm{I}$, are specified.

Figures 10 and 11 illustrate the behaviours of hard and ideally hard materials. For a hard material A increasing monotonically with either increasing or decreasing e but never exceeds a limiting value $A_\infty > A_0$. The model law is uniquely determined once A_0, A_∞ and e_I are specified. For an ideally hard material $A_\infty = \infty$ and e can only vary in the range $[0, e_1]$. The model law is uniquely determined once A_0, e_1 and the parameter τ, $= T$ when $e = 0.99e_1$, have been specified.

In general, of course, we do not expect that the model laws described in § 8 will curve fit the actual response of any material with the same accuracy as it does an inviscid gas, or a solid which obeys Bell's parabolic law. However, it is hoped that by a judicious choice of the free parameters in those laws the broad qualitative features of the behaviour of many materials can be inferred from a knowledge of the behaviour of the model materials.

In § 9 we show that the reflected and transmitted pulses which are generated at a free interface by the arrival of a large amplitude, but shockless, incident wave can readily be calculated analytically when the model stress–strain laws are used. Although the analysis is valid for an arbitrary incoming pulse, the case when this pulse is a centred wave separating two uniform states is discussed in detail. Such waves are produced by impacting materials which soften in compression or by suddenly pulling materials which soften in extension. The cases of perfectly free and perfectly rigid interfaces also receive special study as does the case when the response of the surrounding medium is linear.

Although the mathematical techniques which are described in this paper are motivated by considering large amplitude waves in elastic materials they are directly applicable to any system whose response is governed by the nonlinear wave equation. For example, the problem which is discussed in § 9 is of immediate relevance in transmission line theory where a nonlinear dielectric, such as a ferrite, is often placed in a linear transmission line to produce short rise times. The problem of the reflexion and transmission of pulses at an interface is also of great interest in nonlinear optical devices which use laser beams. Some of these applications will be discussed in future papers.

2. Uniaxial stretching waves in a bounded elastic medium

To fix ideas, we first consider the uniaxial stretching of an elastic bar or string which is bounded by two parallel material planes which are normal to the direction of stretch. The deformation of the medium is referred to a configuration R where the two bounding planes are a distance D apart. In R the medium is in a uniform state. The normal traction on all planes which are orthogonal to the stretch direction is constant, $= T_0$, and the material is at a constant density ρ_0. In the deformations considered, material surfaces which at any time are plane and parallel to the bounding planes remain plane and parallel at all subsequent times. Each such material plane is tagged by its distance X from one of the bounding planes when the material is in the reference state R. Then, the normal traction $T(X, t)$ per unit undeformed area on the plane $X =$ constant at time t is related to its velocity $u(X, t)$, which is normal to the plane, by the equation

$$\frac{\partial T}{\partial X} = \rho_0 \frac{\partial u}{\partial t}. \tag{2.1}$$

The material velocity is given in terms of the current distance

$$x = x(X, t) \tag{2.2}$$

of the plane X from the bounding plane $X = 0$ by

$$u = \partial x/\partial t. \tag{2.3}$$

The material strain e, computed relative to the configuration R, is given by

$$e = \partial x/\partial X - 1. \tag{2.4}$$

According to equations (2.3) and (2.4) u and e are related by the compatibility condition

$$\partial u/\partial X = \partial e/\partial t. \tag{2.5}$$

Equations (2.1) and (2.5) are the Lagrangian statements for the changes in linear momentum and density, which is given in terms of ρ_0 and e by

$$\rho = \rho_0(1+e)^{-1} \tag{2.6}$$

at a particle.

When the dynamic response of the medium is isotropic and homogeneous with respect to R the traction

$$T = \Sigma(e) \tag{2.7}$$

is a known function of the strain e. When (2.7) is inserted in equation (2.1) it reads

$$A^2(e)\frac{\partial e}{\partial X} = \frac{\partial u}{\partial t}, \tag{2.8}$$

where

$$A(e) = \left(\frac{1}{\rho_0}\frac{\mathrm{d}\Sigma}{\mathrm{d}e}\right)^{\frac{1}{2}}. \tag{2.9}$$

Equations (2.5) and (2.8) govern the variations of the kinematic variables $e(X,t)$ and $u(X,t)$. Once these are calculated equation (2.3) can be integrated, subject to appropriate initial conditions, to determine $x(X,t)$.

2.1 *Riemann's representation*

Large amplitude disturbances which are governed by equations (2.5) and (2.8) are best studied by re-writing these equations in a form first proposed by Riemann. To do this it is convenient to use u and a new strain measure

$$c = \int_0^e A(s)\,\mathrm{d}s, \tag{2.10}$$

rather than u and e, as the basic dependent variables. Then, if the equation of state (2.7) is written in the form

$$T = T(c), \tag{2.11}$$

equations (2.5) and (2.8) can be written

$$\frac{\partial c}{\partial t} = A(c)\frac{\partial u}{\partial X} \quad \text{and} \quad \frac{\partial u}{\partial t} = A(c)\frac{\partial c}{\partial X}, \tag{2.12}$$

where the material function

$$A(c) = \frac{1}{\rho_0}\frac{\mathrm{d}T}{\mathrm{d}c} > 0. \tag{2.13}$$

Note that u, c and A all have the dimensions of velocity. If equations (2.12) are subtracted, the equation which is obtained states that the Riemann variable

$$f = \tfrac{1}{2}(c-u) \tag{2.14}$$

is invariant at any one characteristic wavelet, $\alpha(t, X) =$ constant say, at which X varies with t according to the law

$$\mathrm{d}X/\mathrm{d}t|_{\alpha} = A(c). \tag{2.15}$$

Similarly, if equations (2.12) are added it also follows that the Riemann variable

$$g = \tfrac{1}{2}(c+u) \tag{2.16}$$

is invariant at any one characteristic wavelet, $\beta(t, X) =$ constant say, at which X varies with t according to the law

$$\mathrm{d}X/\mathrm{d}t|_{\beta} = -A(c). \tag{2.17}$$

At the $\alpha =$ constant characteristic wavelet

$$\frac{\mathrm{d}x}{\mathrm{d}t} = \frac{\partial x}{\partial t} + \frac{\mathrm{d}X}{\mathrm{d}t}\frac{\partial x}{\partial X} = u + a, \tag{2.18}$$

where, by (2.4), the local sound speed

$$a(c) = (1+e)\,A. \tag{2.19}$$

Similarly, at the $\beta =$ constant characteristic wavelet

$$\mathrm{d}x/\mathrm{d}t = u - a. \tag{2.20}$$

For definiteness in what follows, each characteristic wavelet of the α-wave is tagged so that

$$\text{at the material boundary } X = 0, \quad \alpha = t, \tag{2.21}$$

and each characteristic wavelet of the β-wave is tagged so that

$$\text{at the material boundary } X = D, \quad \beta = t. \tag{2.22}$$

Then, if $f = F(t)$ at $X = 0$, and if $g = G(t)$ at $X = D$, (2.23)

according to the Riemann relations (2.14) to (2.17) for all (t, X) with $0 \leqslant X \leqslant D$

$$f = F(\alpha) \quad \text{and} \quad g = G(\beta), \tag{2.24}$$

so that, by (2.14) and (2.16),

$$c = G(\beta) + F(\alpha) \quad \text{and} \quad u = G(\beta) - F(\alpha). \tag{2.25}$$

The representations (2.25), with $\alpha(t, X)$ and $\beta(t, X)$ determined from conditions (2.15), (2.17), (2.21) and (2.22), hold for any disturbance in the elastic slab. For the purpose of this paper the problem of determining a specific deformation can roughly be divided into two parts:

(i) that of determining the form of the *signal functions* $F(\alpha)$ and $G(\beta)$ carried by the α-wave and β-wave *components* of the disturbance from given initial and boundary data; and

(ii) that of determining the functions $\alpha(t, X)$ and $\beta(t, X)$ so that the state variables can be determined as functions of (t, X).

2.2. *Linear theory: Hooke's law*

For a medium which obeys Hooke's law problem (ii) can always be solved without knowing the signal functions $F(\alpha)$ and $G(\beta)$. For then, because

$$T = T_0 + E_0 e, \tag{2.26}$$

where $E_0 > 0$ is a material constant,

$$A = (E_0/\rho_0)^{\frac{1}{2}} \equiv \text{constant}, = A_0 \quad \text{say}, \tag{2.27}$$

and equations (2.15) and (2.17) integrate, subject to conditions (2.21) and (2.22), to give

$$\alpha = t - \frac{X}{A_0} \quad \text{and} \quad \beta = t + \frac{X-D}{A_0}. \tag{2.28}$$

The statements (2.25) and (2.26) imply that if any deformation in a material which obeys Hooke's law is described in terms of *Lagrangian* coordinates it can always be represented as the superposition of two components which do not intereact. *A non-distorting, non-attenuated, progressing wave* (the α-wave) moving to the right which carries the *signal* $F(\alpha)$ and a similar wave (the β-wave) moving to the left which carries the signal $G(\beta)$. Since the solution to problem (ii) is always given by the expressions (2.28), the whole problem of analysing any deformation in a Hookean material reduces to problem (i) – the determination of the signal functions $F(\alpha)$ and $G(\beta)$ carried by these waves from prescribed boundary and initial data. Since, according to equations (2.26),

$$\text{at } X = 0: \quad t = \alpha = \beta + D/A_0, \tag{2.29}$$

while

$$\text{at } X = D: \quad t = \beta = \alpha + D/A_0, \tag{2.30}$$

the problem of determining $F(\alpha)$ and $G(\beta)$ from prescribed conditions on the variations of u and $c(= A_0 e)$ at $X = 0$ and $X = D$ usually reduces to solving difference equations.

The use of Lagrangian coordinates (X, t) rather than Eulerian coordinates (x, t) greatly simplifies the description of the wave motions which are described in this paper. The first simplification is obvious. When the boundaries of the medium are material planes, as they are throughout most of this paper, they correspond to the fixed coordinate lines $X = 0$ and $X = D$ in the (X, t) plane. By contrast, their images in the (x, t) plane are not usually known *a priori*, but must be calculated as part of the solution. In addition, as we will show, the description of the interactions between the α and β waves is considerably more complex in the (x, t) plane than in the (X, t) plane. This is immediately obvious for a Hookean material. For suppose that the medium was in the reference state R at $t = -\infty$. Then, according to equations (2.3), (2.25) and (2.28)

$$x = X + \hat{G}(\beta) - \hat{F}(\alpha), \tag{2.31}$$

where

$$\hat{F}(\alpha) = \int_{-\infty}^{\alpha} F(s)\,\mathrm{d}s \quad \text{and} \quad \hat{G}(\beta) = \int_{-\infty}^{\beta} G(s)\,\mathrm{d}s. \tag{2.32}$$

Equations (2.28) and (2.31) imply that the characteristic parameters α and β are related to (x, t) by the *implicit* relations

$$\alpha = t - \frac{x}{A_0} + \frac{d(\alpha,\beta)}{A_0} \quad \text{and} \quad \beta = t + \frac{x-D}{A_0} - \frac{d(\alpha,\beta)}{A_0}, \tag{2.33}$$

where the particle displacement

$$d = x - X = \hat{G}(\beta) - \hat{F}(\alpha). \tag{2.34}$$

Consequently, whereas the variations of α and F with (X, t) do not depend on the signal function G the variations of α and F with (x, t) do. In a Hookean material, although the α-wave component and the β-wave component do not interact in (X, t) space they do interact in (x, t) space. Usually the interaction in (x, t) space is neglected and the function $F(t - [X/A_0])$ is *formally* approximated by $F(t - [x/A_0])$. Since

$$\frac{F\left(t - \frac{x}{A_0}\right)}{F(\alpha)} - 1 = \frac{F\left(t - \frac{X}{A_0} - \frac{d}{A_0}\right) - F\left(t - \frac{X}{A_0}\right)}{F(\alpha)} = \frac{d}{A_0}\frac{F'(\alpha)}{F(\alpha)} + O(d^2), \tag{2.35}$$

a *necessary* condition for the error in this approximation

$$\left|\frac{F(t-[x/A_0])}{F(t-[X/A_0])}-1\right| \quad \text{to be} \quad \ll 1 \tag{2.36}$$

is that that amplitude of the particle displacement

$$|d| \ll \lambda_\alpha, \tag{2.37}$$

where

$$\lambda_\alpha = A_0\left|\frac{F(\alpha)}{F'(\alpha)}\right| \tag{2.38}$$

is the local wavelength of the α-wave. Since $|d|$ can increase as the width D of the transmitting medium increases without violating the condition that the stretch e is small enough to use Hooke's law, condition (2.37) can easily be violated.

3. Mathematically equivalent systems

Equations such as (2.5) and (2.8) also govern the nonlinear responses of many other physical systems. For easy reference in what follows, in this section we list two other mechanical systems whose responses can be described by the analyses presented in this paper. These nonlinear systems have electrical and optical analogues.

3.1. *Inviscid gas*

An inviscid gas is an elastic medium whose strain energy is a function of the density and entropy only. In particular, for uniaxial isentropic flows the hydrostatic pressure $p\ (=-T)$ is a function of the stretch $e=(\rho_0/\rho)-1$. For the special case of a polytropic gas

$$\frac{p}{p_0}=\left(\frac{\rho}{\rho_0}\right)^\gamma \quad \text{or, equivalently,} \quad \frac{T}{T_0}=(1+e)^{-\gamma}. \tag{3.1}$$

For a gas Hooke's law (2.26) is often written

$$p=p_0+E_0(1-[\rho_0/\rho]). \tag{3.2}$$

This is often referred to as 'the tangent gas law' or as 'the $\gamma=-1$ gas'.

3.2. *Shear waves*

If the slab of elastic material is incompressible and if the deformation is produced by unidirectional shear forces at the bounding planes the resulting shear deformation in the slab is also described by equations (2.5) and (2.8). Then, however, $T(X,t)$ and $u(X,t)$ are the shear force and material velocity in the direction of shear at the material plane $X=$ constant which has no normal component of velocity. The transverse velocity u and shear strain e are given in terms of the transverse displacement

$$y=y(X,t) \tag{3.3}$$

of any material particle by

$$u=\partial y/\partial t \quad \text{and} \quad e=\partial y/\partial X. \tag{3.4}$$

If the material response is isotropic with respect to R then $\Sigma(e)$ in equation (2.7) must have the special form

$$\Sigma=e\phi(|e|): \tag{3.5}$$

this form insures that

$$T(-e)=-T(e). \tag{3.6}$$

PHILOSOPHICAL TRANSACTIONS OF THE ROYAL SOCIETY A MATHEMATICAL, PHYSICAL & ENGINEERING SCIENCES

The Riemann representation of the deformation given by equations (2.14) to (2.17) is still valid but now the Lagrangian sound speed

$$A = \left[\frac{1}{\rho_0}\frac{\mathrm{d}}{\mathrm{d}|e|}(|e|\phi(|e|))\right]^{\frac{1}{2}} = A(|c|), \tag{3.7}$$

where

$$|c| = \int_0^{|e|} A\,\mathrm{d}s. \tag{3.8}$$

Usually, for no apparent physical reason, in the limit of small strains condition (3.6) is satisfied by assuming that ϕ is an analytic function of $|e|^2 = e^2$ so that $\mathrm{d}\phi/\mathrm{d}|e| = 0$ when $|e| = 0$. One consequence of this assumption, which is not substantiated experimentally, is that shocks cannot form at the front of a transverse wave which is propagating into a region where $e = 0$.

4. Decay of free vibrations

This paper is mainly concerned with an analysis of large amplitude free vibrations in media whose responses are governed by equations of the form (2.5) and (2.8). A simple example of such a vibration occurs in a nonlinear elastic string when its ends $X = 0$ and $X = D$ are suddenly displaced and then held fixed. Another example is the vibration which is set up in an elastic bar, or crystal, when it is suddenly loaded by a normal traction at one of its ends, $X = 0$ say, which is then released to vibrate freely. Here, the other end, $X = D$ is either held fixed or is also allowed to vibrate freely. A good example of a more complicated vibration which can also be described by the analysis occurs in a layer of saturated soil which is bounded by sea water from above and by rock from below when a stretching pulse crosses either of its boundaries. This pulse could be triggered in the rock by a seismic disturbance or by an underground explosion at a point which is deep compared with the depth of the soil–rock interface. Then, the pulse is essentially plane as it traverses the saturated soil.

As an application of our results to gas flows we also consider the vibration which occurs when a gas which was contained at a high pressure between the closed end of a shock tube and a diaphragm is released by bursting the diaphragm. The initial discontinuity at the diaphragm splits into two waves: a constant strength shock wave which moves away from the closed end of the tube and a centred expansion wave which moves towards it. The expansion wave is totally reflected from the closed end of the tube and then, in turn, is partly reflected and partly transmitted at the contact discontinuity, or material plane, which was generated when the diaphragm burst. The transmitted wave finally catches up with the shock where it is partly reflected and partly dissipated. The theory which is developed in this paper will describe some of the main features of the decay of the disturbance between the tube wall, $X = 0$, and the contact discontinuity $X = D$ up until the time when it is not appreciably affected by the energy which is reflected from the shock.

More generally, we consider stretching waves in an elastic slab which is bounded by material planes, or interfaces, $X = 0$ and $X = D$ which are normal to the axis of stretch. Each bounding plane separates the enclosed medium from some other elastic medium which is also being stretched along the same axis. However, each surrounding medium is of semi-infinite extent in the direction of stretch in the sense that its deformation at the interface with the enclosed medium is not significantly influenced by the energy which may be reflected from its other boundary. In

general, the interfaces are *free* surfaces: their motions are not known *a priori*, but must be calculated as part of the solution. The important exception to this configuration which we also consider is when one, or both, of the surrounding media is replaced by a rigid boundary at which the material velocity does not change, or by a perfectly free boundary at which the normal traction does not change. All four of the examples quoted are special cases of this general formulation.

4.1. *Amplitudes of reflected and transmitted pulses at an elastic–elastic interface*

The analysis of free vibrations is divided into two distinct parts. In the first part only the change in the amplitude of a pulse as it moves to and fro from boundary to boundary together with the amplitudes of the transmitted pulses are calculated. No account of the detailed shapes of these pulses is given. This rather crude, but sometimes sufficient, information can be obtained without restricting the forms of the equations of state of the bounded and surrounding media. The results are quite general. In the second part of the paper we give a detailed analysis of some important free vibrations. This problem is much more difficult than that discussed in the first part. To obtain results of any significance the form of the equation of state in the bounded medium must be specified. However, as we show, this form is quite general and can, in fact, be used to correlate the actual stress–strain relations of a wide variety of elastic media with remarkable accuracy.

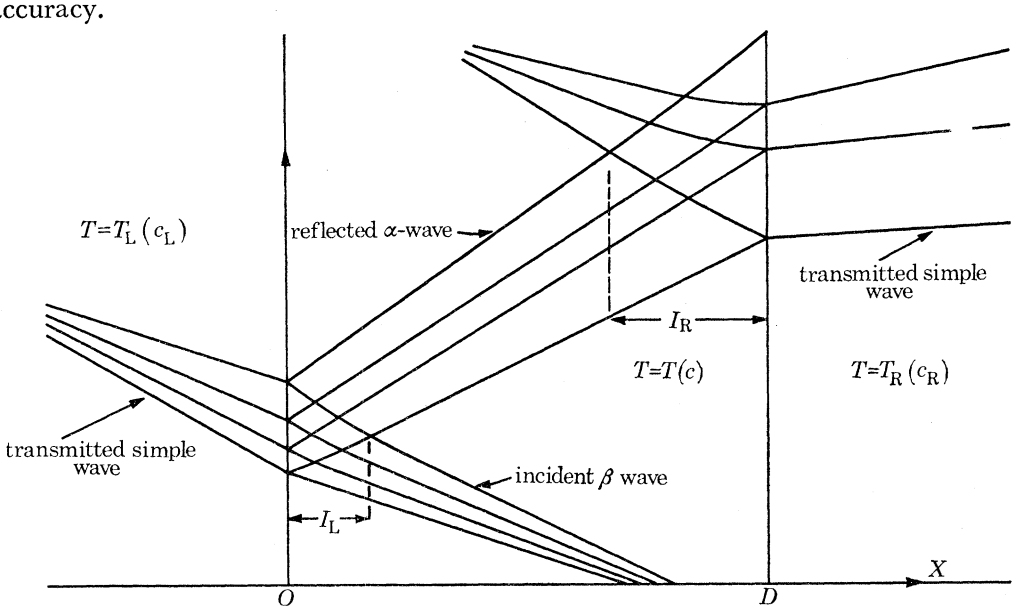

FIGURE 1. The wave system which is set up when an incident pulse is partly reflected and partly transmitted at an interface between two elastic materials.

To make the idea of a free boundary precise, we first calculate the amplitudes of the reflected and transmitted pulses which are generated when a large amplitude shockless pulse is incident at the interface $X = 0$ after traversing the bounded medium. The width of this pulse is taken to be small compared with D. In addition, before its front reaches $X = 0$ the material ahead of it, and behind it, is in equilibrium in the reference configuration R (see figure 1). Under these conditions, since the wave is moving into a region where $f \equiv 0$, according to the relations (2.14) to (2.17), the pulse is a simple wave in which, irrespective of the signal $G(\beta)$ carried by the wave,

$$f = 0 \quad \text{and} \quad u = c = g. \tag{4.1}$$

Since T and e are known if c is known, in the incident pulse all the state variables u, c, T and e are known functions of g. Consequently, since

$$\text{at any particle } X \quad \frac{\partial g}{\partial t} = G'(\beta)\frac{\partial \beta}{\partial t}, \tag{4.2}$$

stationary values of g and all the state variables occur simultaneously in the incident pulse at the arrival of the characteristic wavelets at which the signal function G has stationary values. These stationary values are good measures of the amplitudes of the state variables in the pulse.

As soon as the front of the incident pulse reaches the interface $X = 0$ it produces a reflected α-wave, which moves towards the boundary $X = D$, and a transmitted wave which moves into the surrounding medium (see figure 1). Since the incident pulse is affected by the signal carried by the reflected α-wave, it is no longer a simple wave once its front reaches $X = 0$. Then, in general, the stationary values of u at any X do not occur at the same time as those of T, c and e. However, at the free interface $X = 0$ these stationary values do again occur simultaneously. In fact, they occur at the arrival of the β-wavelet whose passage marked the occurence of the stationary values in the incident pulse. Moreover, these stationary values can easily be determined in terms of the stationary values of g in the incident pulse. This means that the amplitude of the disturbance at the interface can be found if the amplitude of the incident pulse is known.

To establish these results first note that the wave which is transmitted into the surrounding medium to the left of the interface $X = 0$ is also a simple wave. Consequently, if the subscript L denotes the value of a variable in this surrounding medium, so that its equation of state reads

$$T_{\mathrm{L}} = T_{\mathrm{L}}(c_{\mathrm{L}}), \tag{4.3}$$

in the transmitted wave, irrespective of the form of the transmitted signal $G_{\mathrm{L}}(\beta_{\mathrm{L}})$,

$$c_{\mathrm{L}} = u_{\mathrm{L}} = g_{\mathrm{L}}. \tag{4.4}$$

In particular, the relation (4.4) holds at the interface $X = 0$ where, in addition, since the interface is a material plane

$$u = u_{\mathrm{L}} \quad \text{and} \quad T = T_{\mathrm{L}}. \tag{4.5}$$

Conditions (4.3) to (4.5), together with the equations (2.24) and (2.25), imply that

$$\text{at} \quad X = 0, \quad T(c) = T_{\mathrm{L}}(c_{\mathrm{L}}), \tag{4.6}$$

where

$$c = g + f \quad \text{and} \quad c_{\mathrm{L}} = g - f. \tag{4.7}$$

Equations (4.6) and (4.7) provide an implicit equation for the *reflexion function*

$$f = L(g) \quad \text{at} \quad X = 0. \tag{4.8}$$

If equation (4.6) is differentiated, with c and c_{L} given by equations (4.7), it follows that the *local reflexion coefficient*

$$l(g) = L'(g) = \frac{i(g) - 1}{i(g) + 1}, \tag{4.9}$$

where the *local impedance of the interface*

$$i(g) = \frac{\mathrm{d}T_{\mathrm{L}}}{\mathrm{d}c_{\mathrm{L}}} \Big/ \frac{\mathrm{d}T}{\mathrm{d}c} = \rho_{\mathrm{L}0} A_{\mathrm{L}} / \rho_0 A_0 \quad \text{by equation (2.13)}, \tag{4.10}$$

$$= \rho_{\mathrm{L}} a_{\mathrm{L}} / \rho a \quad \text{by equations (2.6) and (2.19)}. \tag{4.11}$$

PHILOSOPHICAL TRANSACTIONS OF THE ROYAL SOCIETY A MATHEMATICAL, PHYSICAL & ENGINEERING SCIENCES

If the interface is perfectly free then, irrespective of the amplitude of the incident pulse,

$$\text{at} \quad X = 0, \quad c = 0 \quad \text{and, by (2.25)}, \quad L \equiv -g. \tag{4.12}$$

This corresponds to $i \equiv 0$ in equation (4.9). If the interface is rigid, then

$$\text{at} \quad X = 0, \quad u = 0 \quad \text{and, by (2.25)}, \quad L \equiv g. \tag{4.13}$$

This corresponds to $i \equiv \infty$. For the special case when the interface separates two media which obey Hooke's law A_{L} and A are constant and i is independent of g.

Since the reflexion function $L(g)$ of the interface is determined by the equations of state of the media it separates

$$\text{at} \quad X = 0, \quad f = L(g), \quad c = g + L(g) \quad \text{and} \quad u = g - L(g), = g_{\mathrm{L}}, \tag{4.14}$$

are known functions of g. Consequently, according to equation (4.9),

$$\text{at} \quad X = 0, \quad \left(\frac{\partial f}{\partial t}, \frac{\partial c}{\partial t}, \frac{\partial u}{\partial t}\right) = \left(\frac{i-1}{i+1}, \frac{2i}{i+1}, \frac{2}{i+1}\right) G'(\beta) \frac{\partial \beta}{\partial t}. \tag{4.15}$$

Equations (4.15) imply the stated result: at the interface stationary values of u and c, and, consequently, of u, c, T and e, occur simultaneously at the arrival of the characteristic wavelet at which G has a stationary value. Moreover, stationary values of f and g_{L}, the signal functions of the reflected and transmitted waves, also occur at this time. If $g = g_1$ denotes a stationary value of $G(\beta)$ in the incident pulse, which corresponds to the stationary values

$$T = T(g_1) \quad \text{and} \quad u = g_1 \tag{4.16}$$

in the traction and velocity, the corresponding stationary values of T and u at the interface (and in the transmitted wave) are

$$T_{\mathrm{L}} = T(g_1 + L(g_1)) \quad \text{and} \quad u_{\mathrm{L}} = g_1 - L(g_1). \tag{4.17}$$

The corresponding stationary value of $F(\alpha)$ and in the reflected wave is

$$f_1 = L(g_1). \tag{4.18}$$

The corresponding stationary value of $G_{\mathrm{L}}(\beta_{\mathrm{L}})$ in the transmitted wave is

$$g_{\mathrm{L}1} = g_1 - L(g_1). \tag{4.19}$$

Once the reflected α-wave has travelled some distance, l_{L} say, from $X = 0$ where it interacts with the incident pulse it moves into a region where, prior to its arrival, the medium is again in equilibrium in the reference configuration R. Consequently, while traversing this region the reflected pulse is a simple wave in which, according to equations (2.14) to (2.17),

$$g = 0 \quad \text{and} \quad c = -u = f. \tag{4.20}$$

Again stationary values of the state variables occur simultaneously and can easily be found from the stationary value of any state variable in the incident pulse. In particular, the stationary values of the traction and particle velocity in the reflected pulse which are associated with the stationary value $u = g_1$ in the incident pulse are

$$T = T(f_1) = T(L(g_1)) \quad \text{and} \quad u = -f_1 = -L(g_1). \tag{4.21}$$

This, then, completes the problem of calculating the amplitude of the state variables in the transmitted and reflected waves, together with their amplitudes at the interface, from the prescribed value of any one state variable in the incident pulse.

4.2. *Multiple reflexions*

Now that the change in the amplitude of a pulse after a single reflexion from a free boundary has been calculated, it is a simple matter to calculate its change in amplitude after multiple reflexions from both free boundaries. To do this we must first define the functions which describe the reflexion properties of the interface $X = D$.

If a subscript R denotes the value of a state variable in the medium to the right of the interface $X = D$, so that the equation of state of this medium reads

$$T_{\mathrm{R}} = T_{\mathrm{R}}(c_{\mathrm{R}}), \tag{4.22}$$

then, by the same reasoning used to analyse conditions at the interface $X = 0$,

$$\text{at} \quad X = D: \quad g = R(f), \tag{4.23}$$

where the reflexion coefficient

$$r(f) = R'(f) = \frac{j(f) - 1}{j(f) + 1}. \tag{4.24}$$

In equation (4.24) the impedance

$$j(f) = \frac{\rho_{\mathrm{R}0} A_{\mathrm{R}}}{\rho_0 A} = \frac{\rho_{\mathrm{R}} a_{\mathrm{R}}}{\rho a} \quad \text{at} \quad X = D. \tag{4.25}$$

For simplicity, let us suppose that g_1 is the only stationary value of G in the incident pulse. Then, according to equations (4.21) and (4.22), at the first return of the pulse to the interface $X = D$ after its first reflexion from $X = 0$ stationary values of f and g, and, consequently, of all the state variables, occur simultaneously. They are

$$f_1 = L(g_1) \quad \text{and} \quad g_2 = R(f_1) = R(L(g_1)). \tag{4.26}$$

g_2 is also the stationary value of g in the pulse during its second approach to the interface $X = 0$. More generally, the stationary value of g in the pulse during its nth approach to the interface $X = 0$ is

$$g_n = R(L(g_{n-1})) \quad \text{for all} \quad n \geqslant 2. \tag{4.27}$$

In addition, outside the interaction regions which border the interfaces $X = 0$ and $X = D$ this pulse is a simple wave in which $f = 0$. (The widths of the interaction regions vary with n.) Similarly, the stationary value of f in the pulse during its nth approach to the interface $X = D$ is

$$f_n = L(R(f_{n-1})) \quad \text{for all} \quad n \geqslant 2, \tag{4.28}$$

where f_1 is given in terms of g_1 by equation (4.26). In this pulse, outside the interaction regions, $g = 0$. At the nth arrival of the pulse

$$\text{at} \quad X = 0, \text{ the stationary values of } (g, f) \text{ are } (g_n, L(g_n)): \tag{4.29}$$

at the nth arrival of the pulse

$$\text{at} \quad X = D, \text{ the stationary values of } (f, g) \text{ are } (f_n, R(f_n)). \tag{4.30}$$

For the special case when all three elastic media obey Hooke's law

$$L(g) = lg \quad \text{and} \quad R(f) = rf, \tag{4.31}$$

where the reflexion coefficients l and r are constant. Then, according to equations (4.27) and (4.28),

$$g_n = (lr)^{n-1} g_1 \quad \text{and} \quad f_n = (lr)^{n-1} f_1, \tag{4.32}$$

where, by equation (4.21),

$$f_1 = l g_1. \tag{4.33}$$

Since l and r are given in terms of the positive impedances i and j by equations (4.9) and (4.24) it immediately follows that both

$$|l| \leqslant 1 \quad \text{and} \quad |r| \leqslant 1. \tag{4.34}$$

The equality sign holds in equations (4.34) if the interface is either perfectly free or rigid. Except for these limiting cases, equations (4.32) and (4.34) predict that both $|g_n|$ and $|f_n|$, and consequently $|u|$ and $|c|$, decrease as n increases.

In some of the processes which can be described by the analyses presented in this paper it is not the nature of the disturbance in the bounded medium which is of primary interest but that of the transmitted pulses. A good example of this occurs in an infinite electrical transmission line. Here, typically, the responses of the surrounding media could be linear and only that of the bounded medium (such as a ferrite) nonlinear. The whole aim of inserting this element into the line is to shape the transmitted wave. For completeness then, we give the stationary values of g_{L} in the pulses which are transmitted to the left of $X = 0$ and the stationary values of f_{R} in the pulses which are transmitted to the right of $X = D$. Since all these pulses are simple waves, once these stationary values are known the corresponding stationary values of all the state variables can readily be determined. The stationary value of g_{L} in the nth transmitted pulse is given by a direct generalization of equation (4.19). It is

$$g_{\mathrm{L}n} = g_n - L(g_n). \tag{4.35}$$

By using a similar argument, it follows that the stationary value of f_{R} in the nth transmitted pulse is

$$f_{\mathrm{R}n} = f_n - R(f_n). \tag{4.36}$$

Up to now, to simplify the discussion, it has been assumed that the disturbance in the elastic slab is generated by the passage of a pulse whose width is small compared with D. This insured that the interaction regions I_{L} and I_{R} did not fill the whole slab. If this restriction is dropped so that the forward and backward waves interact for all X in $0 \leqslant X \leqslant D$ there is no simple wave region in the slab. However, because the transmitted waves are still simple waves, stationary values of g and f and consequently of all the state variables do still occur simultaneously at the boundaries. They are still given by equations (4.29) and (4.30) with the g_n and f_n related by equations (4.27) and (4.28).

It should be noted that the results described in this section have been derived by using purely algebraic manipulations. The results are only strictly valid up until the time when a shock forms and they give no information about the times at which the stationary values occur.

Although in most of this paper we are mainly concerned with exact results, it should perhaps be noted that under certain conditions the results describing conditions in the bounded medium continue to hold to a good approximation even when the bounding media are inhomogeneous so that the transmitted pulses are not simple waves. For it has been shown by Varley & Cumberbatch (1970) that the first of the relations, $c_{\mathrm{L}} = u_{\mathrm{L}}$, in equation (4.4), still continues to hold to a good approximation at the interface $X = 0$ if the widths of the transmitted pulses are small

compared with a length scale defined by the stratification. The relation also holds to a good approximation if the bounding media are viscoelastic and the durations of the pulses are short compared with their relaxation times.

5. Decay of a pulse in fully saturated soil

To illustrate the general results which were established in §4 we consider the decay of a pulse as it moves back and forth in a layer of fully saturated soil which is bounded by sea water from above and by rock from below. The pulse can be thought of as triggered in the rock at a depth below the soil–rock interface which is large compared with D. Then the pulse is essentially plane as it traverses the layer. When the pulse reaches the soil–rock interface after travelling through the rock, because the impedance of the interface is so large, most of its energy is reflected back into the rock and only a small part is carried by the pulse which is transmitted into the soil. It is this transmitted energy which generates the disturbance in the soil and, ultimately, the water above it. For simplicity, *we will assume that for all subsequent reflexions of the pulse, the soil–rock interface acts as a rigid boundary.*

According to Cole (1948) the dynamic pressure–density relation for sea water is well approximated over a wide pressure range by the formula

$$p_{\mathrm{L}} = p_{\mathrm{L}0} + \frac{\rho_{\mathrm{L}0} A_{\mathrm{L}0}^2}{\gamma}\left[\left(\frac{\rho_{\mathrm{L}}}{\rho_{\mathrm{L}0}}\right)^{\gamma} - 1\right], \tag{5.1}$$

where $\rho_{\mathrm{L}0}$ and $A_{\mathrm{L}0}$ are the density and sound speed in the water when it is at uniform pressure $p_{\mathrm{L}0}$. Equation (5.1) also relates the pressure and density in the isentropic flow of an inviscid, polytropic gas. For sea water, typically, the exponent $\gamma = 7.15$; for a gas $\gamma = 1.40$. In terms of the traction T_{L} and the strain e_{L} equation (5.1) reads

$$T_{\mathrm{L}} = T_{\mathrm{L}0} + \frac{\rho_{\mathrm{L}0} A_{\mathrm{L}0}^2}{\gamma}[1 - (1 + e_{\mathrm{L}})^{-\gamma}], \tag{5.2}$$

which, according to equations (2.9) and (2.10), gives

$$1 + e_{\mathrm{L}} = \left(1 - \frac{\gamma - 1}{2}\frac{c_{\mathrm{L}}}{A_{\mathrm{L}0}}\right)^{-2/(\gamma-1)}, \quad A_{\mathrm{L}} = A_{\mathrm{L}0}\left(1 - \frac{\gamma - 1}{2}\frac{c_{\mathrm{L}}}{A_{\mathrm{L}0}}\right)^{(\gamma+1)/(\gamma-1)} \tag{5.3}$$

and

$$T_{\mathrm{L}} = T_{\mathrm{L}0} + \frac{\rho_{\mathrm{L}0} A_{\mathrm{L}0}^2}{\gamma}\left[1 - \left(1 - \frac{\gamma - 1}{2}\frac{c_{\mathrm{L}}}{A_{\mathrm{L}0}}\right)^{2\gamma/(\gamma-1)}\right]. \tag{5.4}$$

Fully saturated soil is an example of a material which hardens in compression. Figure 2 shows a typical relation between stress and strain during its dynamic compression. These results are taken from the experiments of Liahov (1964). In the same figure the relations between stress and strain during the dynamic compression of dry sand and clay silt have also been depicted. These results are due to Allen *et al.* (1957) and Ginsburg (1964). The stress and strain scales have been weighted so that these relations are correlated as closely as possible. During compression all these materials harden in the sense that the local tangent modulus increases until the material becomes almost rigid. During unloading the dry sand and clay silt do not, in general, follow the same stress–strain curve as they do in loading. However, according to Cristescu (1967), if there is no seepage so that the soil remains fully saturated, as it does in the ocean bed, this hysteresis is negligible. Accordingly, in what follows, it is assumed that the dynamic response of the saturated soil is always elastic.

Only pulses which compress the soil relative to its undisturbed state will be considered. If the strain is computed relative to this state then the equation of state of the saturated soil is curve fitted by an expression of the form

$$T = T_0 + 3e_1\rho_0 A_0^2[(1-e/e_1)^{-\frac{1}{3}} - 1]. \tag{5.5}$$

This relation is represented by the full curve in figure 2. The fit is remarkably good for

$$0 \leqslant e/e_1 \leqslant 0.85.$$

For a typical locking strain $e_1 = -\frac{1}{3}\%$ this corresponds to a compressive strain $-e = 0.28\%$. It is shown in §8 that the theoretical stress–strain relation (5.5) is one of a class for which equations (2.12) can be integrated. Although this relation gives a highly idealized approximation to the actual stress–strain relation in the vicinity of the locking strain $e = e_1$, where the local Young's modulus $E = \mathrm{d}T/\mathrm{d}e$ is large but not infinite compared with the modulus $E_0 = \rho_0 A_0^2$ at $e = 0$,

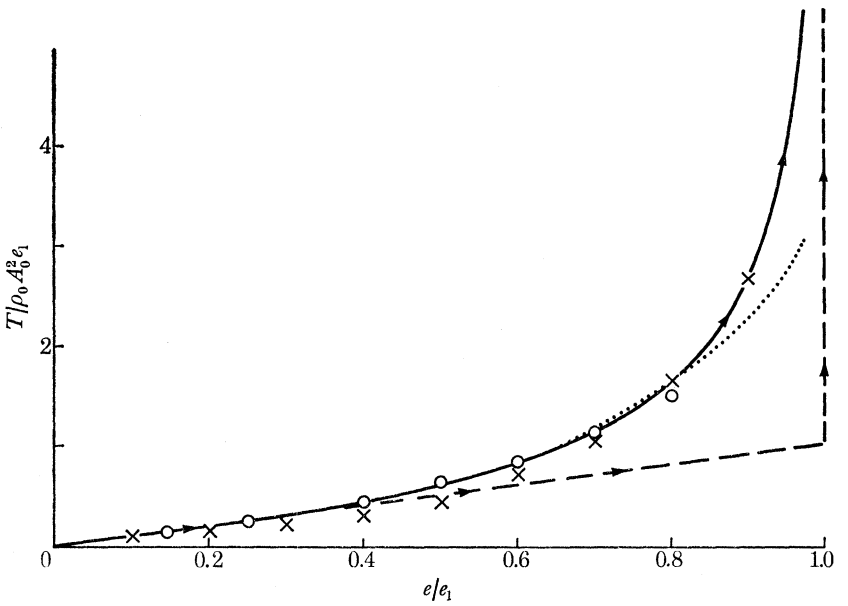

FIGURE 2. Comparison of the experimental stress–strain relations during the dynamic compression of saturated soil, dry sand and clay silt with the theoretical law

$$\frac{T}{\rho_0 A_0^2 e_1} = 3\left[\left(1-\frac{e}{e_1}\right)^{-\frac{1}{3}} - 1\right].$$

———, Theoretical law; × × ×, dry sand (Allen *et al.* 1957); ○○○, saturated soil (Liahov 1964); . . . . ., clay silt (Ginsburg 1964); — —, linear elastic, perfectly hard material.

it does give a much better curve fit than that usually used for locking materials which is depicted by the broken curve in figure 2. Actually it is shown in §6 that the experimental stress–strain curves can be approximated much better by other analytic relations which also lead to mathematically tractable governing equations. However, for an equation of state of the form (5.5) these equations simplify even further. Moreover, for a suitable choice of the parameters e_1 and E_0, this equation of state not only gives a reasonable approximation to the behaviour of saturated soil but also to dry sand and clay silt during compression.

To simplify the algebra, in what follows it is convenient to work with the normalized variables

$$(\bar{u}, \bar{c}, \bar{f}, \bar{g}) = (3e_1 A_0)^{-1}(u, c, f, g). \tag{5.6}$$

Then, when (5.5) holds,

$$\bar{e} = \frac{e}{e_1} = 1-(1-\bar{c})^3, \quad \bar{A} = \frac{A}{A_0} = (1-\bar{c})^{-2} \tag{5.7}$$

and

$$\bar{T} = \frac{T-T_0}{3e_1\rho_0 A_0^2} = \frac{\bar{c}}{1-\bar{c}} = (1-\bar{e})^{-\frac{1}{3}} - 1. \tag{5.8}$$

The corresponding variations of the state variables as functions of $\bar{g}$ in the incident pulse where $\bar{f}=0$ are drawn in the top right quadrant of figure 3. Only variations of $\bar{g}$ over the range $0 \leqslant \bar{g} \leqslant 0.5$ are considered. This corresponds to $\bar{e}$ varying in the range $0 \leqslant \bar{e} \leqslant 0.875$. For larger values of $\bar{e}$ the simple formula (5.8) does not give a good quantitative fit to the experimental data.

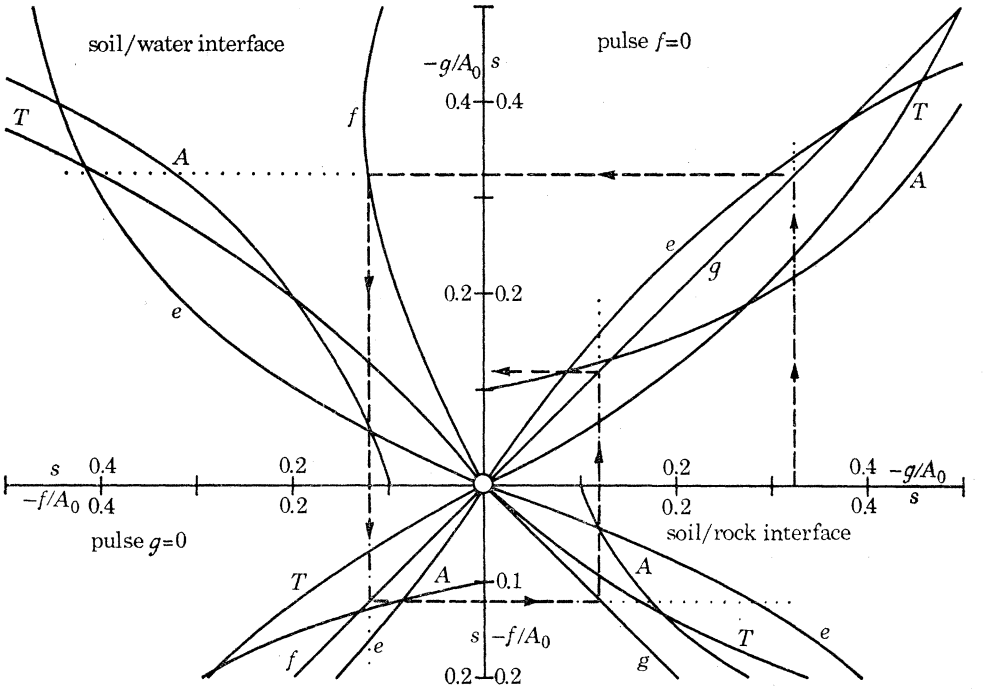

FIGURE 3. Variations of the state variables

$$s = \left[-\frac{f}{A_0}, -\frac{g}{A_0}, 0.1\frac{A}{A_0}, \frac{T_0-T}{\rho_0 A_0^2}, -\tfrac{3}{2}e\%\right]$$

with g in the incident pulse and at the soil/water interface, and with f in the reflected pulse and at the soil/rock interface. To calculate the maximum value of $-f/A_0$ at the soil/water interface given the maximum value of $-g/A_0$ in the incident pulse follow the broken lines. To calculate the corresponding maxima of the state variables s follow the dotted lines. To calculate the maxima of $-f/A_0$ in the reflected pulse and the maxima of $-f/A_0$ and $-g/A_0$ at the soil/rock interface continue to follow the broken lines. To calculate th ecorresponding values of the state variables follow the dotted lines. The maxima value of $-g/A_0$ at the soil/rock interface is identical with that in the pulse during its second approach to the soil/water interface. By making n similar circuits the reduction in the amplitude of the pulse after n reflexions from both interfaces can be calculated.

To obtain the relation between $\bar{f}$ and $\bar{g}$ at the soil–water interface the procedure described in §4 is used. $\bar{T}$ given by the expression (5.8) is equated to $\bar{T}_L$ given by the expression (5.4) with

$$c_L = u \quad \text{and} \quad T_{L0} - T_0. \tag{5.9}$$

This yields, at $X=0$:

$$\bar{T} = \frac{\bar{c}}{1-c} = \frac{i_0}{\delta}\left[\left(1+\frac{\gamma-1}{2\gamma}\delta\bar{u}\right)^{2\gamma/(\gamma-1)} - 1\right], \tag{5.10}$$

where

$$\bar{c} = \bar{g}+\bar{f} \quad \text{and} \quad \bar{u} = \bar{g}-\bar{f}. \tag{5.11}$$

In equation (5.10), $$i_0 = \frac{\rho_{L0} A_{L0}}{\rho_0 A_0} \quad \text{and} \quad \delta = -3\gamma e_1 \frac{A_0}{A_{L0}} > 0. \tag{5.12}$$

When $|\delta\bar{u}| \ll 1$ the relation (5.10) can be approximated by the linear relation

$$\bar{c} = i_0 \bar{u}, \quad \text{or} \quad c = i_0 u, \tag{5.13}$$

which, together with the relations (5.11), imply that

$$\bar{f} = \frac{i_0 - 1}{i_0 + 1} \bar{g}. \tag{5.14}$$

A typical example of the reflexion function $\bar{f} = \bar{L}(\bar{g})$, which results from the relations (5.10) and (5.11), is depicted in the upper left quandrant of figure 3. This corresponds to

$$(\rho_0, \rho_{L0}) = (2, 1)\,\text{g/cm}^3; \quad (A_0, A_{L0}) = (0.2, 1.5)\,\text{km/s}, \quad \text{and} \quad e_1 = -0.333\,\%, \tag{5.15}$$

which, with $\gamma = 7.15$, yields

$$i_0 = 3.750 \quad \text{and} \quad \delta = 0.953 \times 10^{-2}. \tag{5.16}$$

The values (5.15) have been taken from Cristescu (1967) and Hampton & Huck (1968). Because $i_0 > 1$, a small amplitude compression pulse in which $\bar{g} > 0$ is reflected as a compression pulse in which $\bar{f} > 0$. However, its amplitude is cut by almost half and a large part of its energy is transmitted to the water. This contrasts with the situation when the interface is with air. Then, typically,

$$\rho_{L0} = 1.2 \times 10^{-3}\,\text{g/cm}^3, \quad A_{L0} = 0.346\,\text{km/s} \quad \text{and} \quad \gamma = 1.40. \tag{5.17}$$

These values yield $$i_0 = 1.04 \times 10^{-3} \quad \text{and} \quad \delta = 0.813 \times 10^{-2}. \tag{5.18}$$

At this interface, because $i_0 \ll 1$ a small amplitude compression pulse is almost totally reflected as an expansion pulse and little energy is lost to the atmosphere.

According to figure 3 at the soil–water interface $\bar{f}$ at first increases and then begins to decrease as $\bar{g}$ increases. The maximum value of $\bar{f}$ is 0.126 and occurs when the local impedance $i = 1$ at $\bar{g} = 0.394$. This implies that no matter how close $\bar{e}$ is to its limiting value unity in the incident pulse, the maximum strain induced by the reflected pulse outside the interaction regions corresponds to $\bar{e} = 0.330$. The maximum compression at the interface, however, is larger than its maximum in the incident pulse. For example, if the maximum value of $\bar{c}$ in the incident pulse is 0.5, which corresponds to a maximum value of $\bar{e} = 0.875$, then the maximum value of $\bar{c}$ at the interface of 0.615, which corresponds to $\bar{e} = 0.943$.

In addition to the reflexion function, the variations of the state variables $\bar{u}$, $\bar{c}$, $\bar{T}$ and $\bar{e}$ at the soil–water interface are also plotted as functions of $\bar{g}$ in the top left quadrant of figure 3. Their variations in the reflected pulse where $\bar{g} = 0$ are also plotted as functions of $\bar{f}$ in the bottom left quadrant and, finally, as functions of $\bar{f}$ at the soil–rock interface in the bottom right quadrant. Here, because $\bar{u} = 0$,

$$\text{at} \quad X = D, \quad \bar{g} = \bar{f} (\equiv \bar{R}(\bar{f})). \tag{5.19}$$

Figure 3 can readily be used to follow the decay of the disturbance in the soil. To determine f_1, the maximum value of f at the soil–water interface, and g_2, the maximum value of g at the soil–rock interface, from the maximum value of g ($= g_1$) in the incident pulse follow the broken lines. To determine the corresponding values of the state variables at the interface and outside the interaction regions follow the dotted lines. The corresponding values of f_n and g_n are obtained by making n similar circuits.

PHILOSOPHICAL TRANSACTIONS OF THE ROYAL SOCIETY A MATHEMATICAL, PHYSICAL & ENGINEERING SCIENCES

6. Decay of a vibration in a shock tube

As another application of the results which were derived in §4, in this section we describe some of the features of the vibration which results when a perfect gas which is contained at a high pressure between the closed end of a shock tube and a diaphragm is suddenly released when the diaphragm bursts. The broad features of the initial motion are well known and are discussed, for example, by Courant & Friedrichs (1948). They are illustrated in figure 4. Initially the discontinuity at the diaphragm produces a constant strength shock wave which moves away from the closed end of the tube and a centred expansion wave which moves towards it. The gas in the region between these waves is initially in uniform motion and is at a uniform pressure. The temperature and sound speed in this region, however, are only piecewise uniform. They are discontinuous at the contact surface, or material plane, $X = D$ which was produced at the cross-section occupied by the diaphragm when it burst. Initially, this contact discontinuity, which separates particles which have been processed by the shock from those which have not, moves away from the closed end of the tube with the constant speed of the flow.

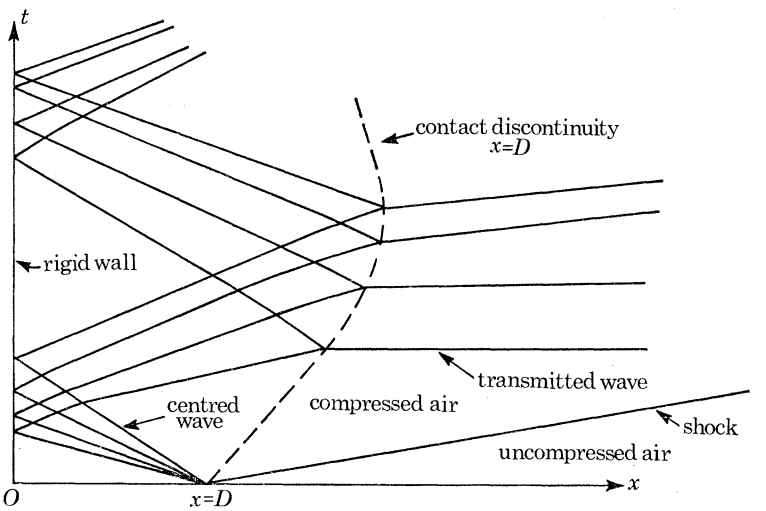

Figure 4. Wave motion produced in a shock tube by removing a membrane separating gas under high pressure from air at atmospheric pressure.

Once the expansion wave reaches the end $X = 0$ it is totally reflected as an expansion wave. Then it catches up with the contact discontinuity where it is partially reflected and partially transmitted. Since the transmitted wave is moving into a uniform region it remains a simple wave until it too is partially reflected by the shock. The analysis presented below is only valid up until the time when no shocks form in the region $0 \leqslant X \leqslant D$, or when the energy which is reflected from the transmitted shock has a significant effect on the disturbance in this region.

For simplicity, only the special case when the initial temperatures of the gases on both sides of the diaphragm are equal will be discussed. Then, if (p_0, ρ_0) denote the pressure and density in the contained gas before the diaphragm is ruptured and if (p_∞, ρ_∞) denote their values in the gas to the right of the diaphragm, the equilibrium sound speeds in the two gases are equal and are given by

$$a_0 = \left(\frac{\gamma p_0}{\rho_0}\right)^{\frac{1}{2}} = \left(\frac{\gamma p_\infty}{\rho_\infty}\right)^{\frac{1}{2}}. \tag{6.1}$$

In what follows, to avoid messy algebra, it is convenient to measure all pressures in units of p_0 and all velocities in units of a_0. Then, with this convention, the usual shock conditions (see Courant & Friedrichs 1948) imply that in the uniform flow behind the shock

$$u_{R0} = \frac{2}{\gamma+1}\frac{M^2-1}{M}, \quad a_{R0} = \left[1+\frac{2\gamma}{\gamma+1}(M^2-1)\right]^{\frac{1}{2}}\left[1-\frac{2}{\gamma+1}\frac{M^2-1}{M^2}\right]^{\frac{1}{2}} \tag{6.2}$$

and

$$p_{R0} = p_\infty\left[1+\frac{2\gamma}{\gamma+1}(M^2-1)\right], \tag{6.3}$$

where M is the shock speed. In the gas between the wall $X = 0$ and the contact discontinuity $X = D$,

$$c = \frac{2}{\gamma-1}[1-p^{(\gamma-1)/2\gamma}]. \tag{6.4}$$

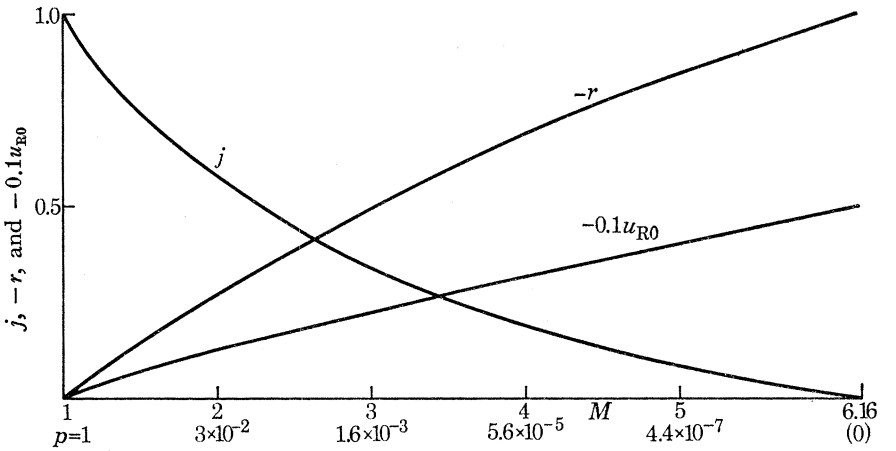

FIGURE 5. Variations of the impedance j, the reflexion coefficients r and the initial speed u_{R0} of a contact discontinuity as a function of M, the Mach number of the shock which is produced when a diaphragm in a shock tube is ruptured. p_∞ denotes the pressure ratio across the diaphragm.

To determine M in terms of the pressure ratio $p_\infty \leqslant 1$ across the diaphragm note that in the centred expansion wave

$$\text{where} \quad f = 0, u = c \quad \text{and, consequently,} \quad p = [1-\tfrac{1}{2}(\gamma-1)\,u]^{2\gamma/(\gamma-1)}. \tag{6.5}$$

Since this expansion wave must also border the uniform region where $p = p_{R0}$ and $u = u_{R0}$, inserting the expressions given by equations (6.2) for these variables in equation (6.5) yields

$$p_\infty = \left[1+\frac{2\gamma}{\gamma+1}(M^2-1)\right]^{-1}\left[1-\frac{\gamma-1}{\gamma+1}\frac{M^2-1}{M}\right]^{2\gamma/(\gamma-1)}. \tag{6.6}$$

This relation is plotted in figure 5. As p_∞ increases in the range $0 \leqslant p_\infty \leqslant 1$, when $\gamma = 1.40$, M decreases monotonically in the range $1 \leqslant M \leqslant 6.16$.

6.1. *Reflexion from a rigid wall*

According to equations (6.4) and (6.5) in the centred expansion wave

$$a = p^{(\gamma-1)/2\gamma} = 1-\tfrac{1}{2}(\gamma-1)\,g \quad \text{and} \quad u = g. \tag{6.7}$$

Consequently, the flow only remains subsonic in that part of the wave where g varies in the range

$$0 \leqslant g < 2/(\gamma+1). \tag{6.8}$$

Only that part of the wave where g varies in this range moves towards the closed end of the tube. There,

$$\text{at} \quad X = 0, \quad \text{where} \quad u = 0, \quad f = g\,(\equiv L(g)), \tag{6.9}$$

and so, according to equations (2.16) and (6.4),

$$\text{at} \quad X = 0, \quad c = 2g \quad \text{and} \quad p = [1-(\gamma-1)\,g]^{2\gamma/(\gamma-1)}. \tag{6.10}$$

Since g can only vary in the range (6.8) at the wall, the smallest value of p which can occur during the first incidence is $[(3-\gamma)/(\gamma+1)]^{2\gamma/(\gamma-1)}$, $= 0.058$ when $\gamma = 1.4$. This corresponds to a change in density by a factor 0.011.

6.2. *Reflexion from a contact discontinuity*

To determine the reflexion function $g = R(f)$ we follow the same procedure which was used in §4 with the minor exception that the simple wave which is transmitted at the contact discontinuity is now moving into a region where $u = u_{\mathrm{R0}}$. The gas in this region, between the contact discontinuity and the constant strength shock, is not at the same entropy as that in the region $0 \leqslant X \leqslant D$. Its equation of state is

$$c_{\mathrm{R}} = \frac{2}{\gamma-1}\,a_{\mathrm{R0}}\left[1-\left(\frac{p_{\mathrm{R}}}{p_{\mathrm{R0}}}\right)^{(\gamma-1),2\gamma}\right]. \tag{6.11}$$

In the transmitted simple wave, since

$$g_{\mathrm{R}} = 0, \quad u_{\mathrm{R}} = u_{\mathrm{R0}} + \frac{2}{\gamma-1}\,a_{\mathrm{R0}}\left[\left(\frac{p_{\mathrm{R}}}{p_{\mathrm{R0}}}\right)^{(\gamma-1)/2\gamma} - 1\right]. \tag{6.12}$$

Consequently, since $u_{\mathrm{R}} = u$ and $p_{\mathrm{R}} = p$,

$$\text{at} \quad X = D, \quad u = g - f = u_{\mathrm{R0}} + \frac{2}{\gamma-1}\,a_{\mathrm{R0}}\left[\left(\frac{p}{p_{\mathrm{R0}}}\right)^{(\gamma-1)/2\gamma} - 1\right]. \tag{6.13}$$

In addition, according to equation (6.4),

$$c = g + f = \frac{2}{\gamma-1}\,[1-p^{(\gamma-1)/2\gamma}]. \tag{6.14}$$

Equations (6.9) and (6.10) determine g and f as functions of p at $X = D$. Elimination of p from these equations yields the result that

$$\text{at} \quad X = D\text{:} \quad g = r(p_\infty)f + u_{\mathrm{R0}}(p_\infty)\;(\equiv R(f)), \tag{6.15}$$

so that g and f are linearly related at a contact surface. Since the local reflexion coefficient r is constant, so is the local impedance $j = (1+r)/(1-r)$. According to equation (4.25), this implies that

$$j = \frac{\rho_{\mathrm{R}} a_{\mathrm{R}}}{\rho a}, \quad = \left(\frac{\rho_{\mathrm{R}}}{\rho}\right)^{\frac{1}{2}} \quad \text{for a gas,} \quad \equiv \left(\frac{\rho_{\mathrm{R0}}}{\rho_0}\right)^{\frac{1}{2}} \quad \text{at} \quad X = D. \tag{6.16}$$

Since

$$\begin{aligned}\left(\frac{\rho_{\mathrm{R0}}}{\rho_0}\right) &= a_{\mathrm{R0}}^{-1}(p_{\mathrm{R0}})^{(\gamma-1)/2\gamma} \\ &= \left[1-\frac{\gamma-1}{\gamma+1}\,\frac{M^2-1}{M}\right]\left[1+\frac{2\gamma}{\gamma+1}\,(M^2-1)\right]^{-\frac{1}{2}}\left[1-\frac{2}{\gamma+1}\,\frac{M^2-1}{M^2}\right]^{-\frac{1}{2}} \\ &\leqslant 1 \quad \text{for} \quad 1 \leqslant M \leqslant 6.16,\end{aligned} \tag{6.17}$$

the reflexion coefficient $r \leqslant 0$ so that the wave is partially recompressed during its reflexion from the contact discontinuity.

The variations of r, j and u_{R0} with M_∞ are plotted in figure 5. As p_∞ increases in the range $0 \leqslant p_\infty \leqslant 1$, r increases monotonically in the range $-1 \leqslant r \leqslant 0$ and u_{R0} decreases monotonically in the range $0 \leqslant u_{R0} \leqslant 5$. Once g has been determined from f by equation (6.13) the variations of u, p and the temperatures T and T_R with f at the contact discontinuity can be determined from the formulae

$$u = g - f, \quad p = [1 - \tfrac{1}{2}(\gamma - 1)(g + f)]^{2\gamma/(\gamma-1)}, \quad T = T_0[1 - \tfrac{1}{2}(\gamma - 1)(g + f)]^2 \tag{6.18}$$

and

$$T_R = \rho_0 T/\rho_{R0} \, (\geqslant T).$$

These variations are depicted in figure 5 for selected values of the parameter p_∞. Again we note that the results are only valid if no shocks form in the region $0 \leqslant X \leqslant D$.

Although the flow variables do not attain stationary values in a centred expansion wave, the results which are established in §4 can still be used to describe the broad features of the decay of the disturbance in the region $0 \leqslant X \leqslant D$. For example, as the wave moves back and forth from rigid wall to contact discontinuity periods over which the gas is in a uniform state occur at both boundaries (see figure 4). These uniform states can readily be calculated. In the first uniform state at the contact discontinuity, which occurs just after the diaphragm bursts, $f = 0$ and $g = u_R$. In the first uniform state at the wall, which occurs after the centred expansion wave is totally reflected, $f = g = u_R$. More generally, in the nth uniform states at $X = 0$ and $X = D$, g and f are given by equations (4.33) and (4.34) with f_n and g_n determined by equations (4.31) and (4.32) with $L(g)$ given by equation (6.7), with $R(f)$ given by equation (6.15), and with

$$g_1 = f_1 = u_{R0}. \tag{6.19}$$

When these calculations are performed they yield the results that

$$\text{in the } n\text{th uniform state at } X = 0, \quad g = f = (1 + r)^{n-1} u_{R0} \tag{6.20}$$

for $n \geqslant 2$, while

$$\text{in the } n\text{th uniform state at } X = D, \quad g = (1 + r) f = (1 + r)^{n-1} u_{R0}. \tag{6.21}$$

The corresponding uniform values of the state variables at the contact discontinuity can be found from equations (6.18). In particular, in the nth uniform state at $X = D$ for $n \geqslant 2$

$$u = rf = r(1 + r)^{n-2} u_{R0} \quad \text{and} \quad c = (2 + r) f = (2 + r)(1 + r)^{n-2} u_{R0}. \tag{6.22}$$

Since $-1 \leqslant r \leqslant 0$, according to equation (6.22), during its first arrival at the contact discontinuity the expansion wave decelerates the flow, reverses it, and leaves it with a uniform velocity ru_{R0} (< 0) until it is again processed by the wave. After this first arrival

$$c = (2 + r) u_{R0} > u_{R0}$$

so that the gas is expanded more than it was after being processed by the centred expansion wave. From then on, however, c decreases and the gas is compressed, while u remains negative and decreases in amplitude. Ultimately, a shock forms.

7. Determination of the signal functions $F(t)$ and $G(t)$

In §4 it was shown how to determine the current values of the state variables at the free surface $X = 0$ from the current value of g there, and the values of the state variables at the free surface $X = D$ from the value of f there. It follows that the variations of the state variables with t at both boundaries can be determined from this analysis if the variations of g with t at $X = 0$ and of f with t at $X = D$ can be found. In general, this is a formidable mathematical problem which can only be solved analytically for very special media which are undergoing very special deformations. The main aim of this and succeeding sections is to introduce a class of equations of state for which this problem can be considerably simplified analytically and in many situations solved completely. It is shown in §8 that these equations of state can be used to curve fit the experimental stress–strain curves of a wide variety of media over a wide range of strain.

To motivate the choice of the form which $A(c)$ takes for this class of media it is best to use the characteristic parameters (α, β) as the basic independent variables. Then, according to equations (2.15) and (2.17), $X(\alpha, \beta)$ and $t(\alpha, \beta)$ satisfy the equations

$$\frac{\partial X}{\partial \alpha} = -A(c)\frac{\partial t}{\partial \alpha} \quad \text{and} \quad \frac{\partial X}{\partial \beta} = A(c)\frac{\partial t}{\partial \beta}, \tag{7.1}$$

where, by equation (2.25),

$$c = F(\alpha) + G(\beta). \tag{7.2}$$

When X is eliminated from equations (7.1), they yield the hodograph equation

$$\frac{\partial^2 t}{\partial \alpha\, \partial \beta} + \tfrac{1}{2}A^{-1}\frac{\mathrm{d}A}{\mathrm{d}c}\left[\frac{\partial c}{\partial \alpha}\frac{\partial t}{\partial \beta} + \frac{\partial c}{\partial \beta}\frac{\partial t}{\partial \alpha}\right] = 0 \tag{7.3}$$

for $t(\alpha, \beta)$. This equation can either be written in the form

$$\frac{\partial}{\partial \beta}\left(A^{\frac{1}{2}}\frac{\partial t}{\partial \alpha}\right) + \tfrac{1}{2}A^{-\frac{1}{2}}\frac{\mathrm{d}A}{\mathrm{d}c}\frac{\partial t}{\partial \beta}F'(\alpha) = 0, \tag{7.4}$$

or in the form

$$\frac{\partial}{\partial \alpha}\left(A^{\frac{1}{2}}\frac{\partial t}{\partial \beta}\right) + \tfrac{1}{2}A^{-\frac{1}{2}}\frac{\mathrm{d}A}{\mathrm{d}c}\frac{\partial t}{\partial \alpha}G'(\beta) = 0, \tag{7.5}$$

where a prime denotes differentiation.

The media which are studied in what follows are defined by the property that $A(c)$ satisfies an equation of the form

$$\mathrm{d}A/\mathrm{d}c = \mu A^{\frac{1}{2}} + \nu A^{\frac{3}{2}}, \tag{7.6}$$

where μ and ν are material constants. For any such medium, if equations (7.1) are noted, it follows that equations (7.4) and (7.5) can be written

$$2\frac{\partial}{\partial \beta}\left(A^{\frac{1}{2}}\frac{\partial t}{\partial \alpha}\right) + F'(\alpha)\frac{\partial}{\partial \beta}(\mu t + \nu X) = 0 \tag{7.7}$$

and

$$2\frac{\partial}{\partial \alpha}\left(A^{\frac{1}{2}}\frac{\partial t}{\partial \beta}\right) + G'(\beta)\frac{\partial}{\partial \alpha}(\mu t - \nu X) = 0. \tag{7.8}$$

These equations integrate to give

$$2A^{\frac{1}{2}}\frac{\partial t}{\partial \alpha} + [\mu(t-\alpha) + \nu X]F'(\alpha) = m(\alpha) \tag{7.9}$$

and

$$2A^{\frac{1}{2}}\frac{\partial t}{\partial \beta} + [\mu(t-\beta) + \nu(D-X)]G'(\beta) = n(\beta). \tag{7.10}$$

The functions $m(\alpha)$ and $n(\beta)$ are 'constants' of integration in the integration of the characteristic relations (7.7) and (7.8). In fact

$$m(t) = A^{\frac{1}{2}} \quad \text{at} \quad X = 0 \quad \text{where} \quad t = \alpha \tag{7.11}$$

and

$$n(t) = A^{\frac{1}{2}} \quad \text{at} \quad X = D \quad \text{where} \quad t = \beta. \tag{7.12}$$

This identification follows from equations (7.9) and (7.10) and the results that

$$2\frac{\partial t}{\partial \alpha} = \frac{\mathrm{D}t}{\mathrm{D}\alpha} \text{ at constant } X, \text{ while } 2\frac{\partial t}{\partial \beta} = \frac{\mathrm{D}t}{\mathrm{D}\beta} \text{ at constant } X. \tag{7.13}$$

To prove these latter results, which in fact hold for any $A(c)$, note, for example, that

$$\begin{aligned}\frac{\mathrm{D}t}{\mathrm{D}\alpha} &= \frac{\partial t}{\partial \alpha} + \frac{\mathrm{D}\beta}{\mathrm{D}\alpha}\frac{\partial t}{\partial \beta} \\ &= \frac{\partial t}{\partial \alpha} + A^{-1}\frac{\mathrm{D}\beta}{\mathrm{D}\alpha}\frac{\partial X}{\partial \beta} \text{ by the second of equations (7.1)} \\ &= \frac{\partial t}{\partial \alpha} - A^{-1}\frac{\partial X}{\partial \alpha} = 2\frac{\partial t}{\partial \alpha} \text{ by the first of equations (7.1).}\end{aligned}$$

It follows from equations (7.9), (7.10) and (7.13) that at any constant X

$$A^{\frac{1}{2}}\mathrm{D}t/\mathrm{D}\alpha + [\mu(t-\alpha) + \nu X]\,F'(\alpha) = m(\alpha) \tag{7.14}$$

and

$$A^{\frac{1}{2}}\mathrm{D}t/\mathrm{D}\beta + [\mu(t-\beta) + \nu(D-X)]\,G'(\beta) = n(\beta). \tag{7.15}$$

When all the functions $F(\alpha)$, $G(\beta)$, $m(\alpha)$ and $n(\beta)$ are known, and when A has been determined as a function of F and G from equations (7.2) and (7.6), equations (7.14) and (7.15) provide two nonlinear ordinary differential equations for the variations of α and β with t at any X. Once these variations have been calculated the variations of F and G, and consequently of all the state variables, with t at any X are known. In § 9 we show how to calculate the functions F, G, m and n for the free boundary problems outlined in § 4. Before doing this, however, we first discuss the various material responses which can be described by an equation of state which satisfies equation (7.6).

8. Material behaviours which can be described by equations of state for which $\mathrm{d}A/\mathrm{d}c = \mu A^{\frac{1}{2}} + \nu A^{\frac{3}{2}}$

In what follows T will denote the traction measured relative to the traction in the reference state.

8.1. *Local curve fit*

Although we are primarily concerned with large amplitude deformations, to illustrate the use of the model equations of state for which $A(c)$ satisfies equation (7.6) we show how the parameters μ and ν should be chosen to locally curve fit any prescribed behaviour in the vicinity of some reference state. More precisely, if the prescribed relation between stress and strain in some neighbourhood of $e = 0$ takes the form

$$T = \rho_0 A_0^2[e + pe^2 + qe^3 + O(e^4)], \tag{8.1}$$

then the equation of state obtained by integrating equation (7.6) with

$$\mu = \tfrac{1}{2}p\frac{7q-6}{q}A_0^{-\frac{1}{2}}, \quad \nu = \tfrac{1}{2}p\frac{6-5q}{q}A_0^{-\frac{3}{2}} \quad \text{and} \quad A(0) = A_0 \tag{8.2}$$

has a Taylor series representation which agrees with the expansion (8.1) up to terms $O(e^4)$. This result follows by direct computation using equations (2.7), (2.9), (2.10) and (7.6). The only exception to this result is when $p = 0$, so that $e = 0$ is a point of inflexion. Consequently, except for this case, the model equations of state can be used to locally approximate any given equation of state, at points where the stress can be expanded as a Taylor series in the strain, to within an error $O[e^4]$. This choice is appropriate, for example, when investigating small amplitude deformations which involve weak shocks, or resonant vibrations of crystals, or other small amplitude deformations where the effect of locally small nonlinearity can accumulate to produce first-order effects. For example, for a gas

$$T = \frac{\rho_0 A_0^2}{\gamma}[1-(1+e)^{-\gamma}] = \rho_0 A_0^2[e - \tfrac{1}{2}(\gamma+1)\,e^2 + \tfrac{1}{6}(\gamma+1)\,(\gamma+2)\,e^3 + O(e^4)], \tag{8.3}$$

so that, by equations (8.2),

$$\mu = -\frac{1}{4}\frac{7\gamma^2+21\gamma-22}{\gamma+2}A_0^{-\frac{1}{2}}, \quad \text{and} \quad \nu = \frac{1}{4}\frac{5\gamma^2+15\gamma-26}{\gamma+2}A_0^{-\frac{3}{2}}. \tag{8.4}$$

$$\left.\begin{aligned} &\text{When} \quad \gamma = 1.4, \quad \mu = -1.55A_0^{-\frac{1}{2}} \quad \text{and} \quad \nu = 0.35A_0^{-\frac{3}{2}}, \\ &\text{when} \quad \gamma = \tfrac{5}{3}, \quad \mu = -2.21A_0^{-\frac{1}{2}} \quad \text{and} \quad \nu = 0.88A_0^{-\frac{3}{2}}. \end{aligned}\right\} \tag{8.5}$$

8.2. *Global curve fit*

The constants μ and ν can also be chosen so that the corresponding model stress–strain relations approximate other specified stress–strain relations over a finite range of strain. These latter relations could either be specified analytically, as for a gas, or graphically, as for saturated soil. The purpose of curve fitting these exact or experimental relations (which henceforth will be denoted by the subscript E) by the model relations is that many problems can be solved exactly for the latter but not for the former. In practice, most of the stress–strain relations for solids are determined from experimental data. In general, away from singular points, this data can be curve fitted by any one of a host of analytic expressions. *The class of analytic expressions used here has the considerable advantage that the resulting equations can be integrated in full generality.* Before a full account of the material response which can be modelled is given, to illustrate the curve-fitting procedure two examples will be discussed in some detail.

First we note that the equation of state of a gas, given by equation (8.3), can be well approximated by the model equation of state over a range of strain where the density changes by a factor of 10! If the reference state R is chosen as the state where the density ρ_0 is a maximum (as it was in the shock tube problem) this corresponds to ρ and e varying in the range

$$0.1\rho_0 \leqslant \rho \leqslant \rho_0 \quad \text{and} \quad 0 \leqslant e \leqslant 9. \tag{8.6}$$

There are two families of solutions to equation (7.6) which are given by different analytic expressions. The family which gives the best fit to $A_{\mathrm{E}}(c)$ for a gas is the one for which

$$\frac{A}{A_0} = \theta_2 \tan^2\left(\theta_0 + \theta_1 \frac{c}{A_0}\right), \tag{8.7}$$

where

$$A_0^{\frac{1}{2}}\mu = 2\theta_1\theta_2^{\frac{1}{2}} \quad \text{and} \quad A_0^{\frac{3}{2}}\nu = 2\theta_1\theta_2^{-\frac{1}{2}}. \tag{8.8}$$

Since, according to equations (2.10),

$$\frac{\mathrm{d}T}{\mathrm{d}c} = \rho_0 A \quad \text{and} \quad \frac{\mathrm{d}e}{\mathrm{d}c} = A^{-1}, \tag{8.9}$$

when (8.7) holds
$$\frac{T}{\rho_0 A_0^2} = t_0 + \theta_1^{-1}\theta_2\left[\tan\left(\theta_0 + \theta_1\frac{c}{A_0}\right) - \theta_1\frac{c}{A_0}\right], \tag{8.10}$$

and
$$e = e_0 - (\theta_1\theta_2)^{-1}\left[\cot\left(\theta_0 + \theta_1\frac{c}{A_0}\right) + \theta_1\frac{c}{A_0}\right]. \tag{8.11}$$

When it is specified that the model equation of state must model the reference state *exactly*, without loss of generality, the constants of integration in the expressions (8.10) and (8.11) have the values
$$\theta_2 = \cot^2\theta_0, \quad t_0 = -\theta_1^{-1}\cot\theta_0 \quad \text{and} \quad e_0 = \theta_1^{-1}\tan\theta_0. \tag{8.12}$$

Then,
$$\text{when} \quad c = 0, \quad A = A_0 \quad \text{and} \quad T = e = 0. \tag{8.13}$$

When $\gamma = 1.4$, a good fit† to the stress–strain relation for a gas when ρ varies over the range given by equation (8.6), and when it is specified that conditions (8.13) must hold, is when
$$\theta_0 = 0.8928, \quad \theta_1 = -0.3248, \quad \theta_2 = 0.6479, \tag{8.14}$$

while
$$t_0 = 2.4834 \quad \text{and} \quad e_0 = -3.8343.$$

TABLE 1. COMPARISON OF EXACT AND APPROXIMATE VALUES OF $A(c)$, $p(c)$ AND $\rho(c)$ FOR A GAS WITH AN EXPONENT $\gamma = 1.4$

ρ varies in the range $0.1\rho_0 \leqslant \rho \leqslant \rho_0$ and approximate values correspond to $A = 0.64787A_0\tan^2(0.89278 - 0.32482c/A_0)$.

c/A_0	A_E/A_0	A/A_0	p_E/p_0	p/p_0	ρ_E/ρ_0	ρ/ρ_0
0.0	1.000	0.999	1.000	0.990	1.000	1.007
0.1	0.886	0.875	0.868	0.859	0.904	0.909
0.2	0.783	0.768	0.751	0.746	0.815	0.818
0.3	0.690	0.674	0.648	0.644	0.734	0.735
0.4	0.606	0.592	0.558	0.555	0.659	0.658
0.5	0.531	0.520	0.478	0.478	0.590	0.588
0.6	0.464	0.456	0.409	0.409	0.528	0.525
0.7	0.405	0.399	0.348	0.350	0.470	0.467
0.8	0.351	0.349	0.295	0.297	0.418	0.415
0.9	0.304	0.304	0.249	0.252	0.371	0.368
1.0	0.262	0.264	0.210	0.212	0.328	0.326
1.1	0.225	0.228	0.176	0.178	0.289	0.288
1.2	0.193	0.196	0.146	0.148	0.254	0.253
1.3	0.164	0.168	0.122	0.123	0.222	0.222
1.4	0.139	0.142	0.100	0.101	0.193	0.194
1.5	0.118	0.119	0.0824	0.0827	0.168	0.169
1.6	0.0989	0.0992	0.0672	0.0674	0.145	0.146
1.7	0.0827	0.0814	0.0546	0.0548	0.125	0.126
1.8	0.0687	0.0656	0.0440	0.0446	0.107	0.107
1.845	0.0631	0.0591	0.0398	0.0406	0.100	0.0995

With these values,
$$\mu = -0.5221A_0^{-\frac{1}{2}} \quad \text{and} \quad \nu = -0.8006A_0^{-\frac{3}{2}}. \tag{8.15}$$

The approximate values of $A(c)$, $p(c)$ $(= p_0[1 - \gamma T/\rho_0 A_0^2])$ and $\rho(c)$ are compared with their exact values in table 1. The maximum error is about $1\frac{1}{2}$ %.

For a monatomic gas with $\gamma = \frac{5}{3}$, a good fit is obtained when
$$\left.\begin{aligned} \theta_0 = 0.8420, \quad \theta_1 = -0.3813, \quad \theta_2 = 0.8081, \\ \text{while} \qquad t_0 = 2.3788 \quad \text{and} \quad e_0 = -2.9069. \end{aligned}\right\} \tag{8.16}$$

† How to choose the parameters to obtain the 'best fit' will depend on the flow, or deformation, which is being investigated.

TABLE 2. COMPARISON OF EXACT AND APPROXIMATE VALUES OF $A(c)$, $p(c)$ AND $\rho(c)$ FOR A GAS WITH AN EXPONENT $\gamma = \frac{5}{3}$

ρ varies in the range $0.1\rho_0 \leqslant \rho \leqslant \rho_0$ and approximate values correspond to $A = 0.80811A_0 \tan^2 (0.84204 - 0.38133c/A_0)$.

c/A_0	A_E/A_0	A/A_0	p_E/p_0	p/p_0	ρ_E/ρ_0	ρ/ρ_0
0.0	1.000	1.014	1.000	0.992	1.000	1.010
0.1	0.873	0.870	0.844	0.835	0.903	0.912
0.2	0.759	0.747	0.708	0.701	0.813	0.819
0.3	0.656	0.641	0.590	0.585	0.729	0.732
0.4	0.564	0.549	0.489	0.486	0.651	0.652
0.5	0.482	0.470	0.402	0.401	0.579	0.578
0.6	0.410	0.400	0.328	0.329	0.512	0.510
0.7	0.345	0.340	0.265	0.268	0.451	0.448
0.8	0.289	0.286	0.212	0.216	0.394	0.392
0.9	0.240	0.240	0.168	0.172	0.343	0.341
1.0	0.198	0.199	0.132	0.135	0.296	0.295
1.1	0.161	0.163	0.102	0.105	0.254	0.253
1.2	0.130	0.132	0.0778	0.0805	0.216	0.216
1.3	0.103	0.105	0.0584	0.0608	0.182	0.183
1.4	0.0809	0.0819	0.0432	0.0452	0.152	0.153
1.5	0.0625	0.0619	0.0313	0.0333	0.125	0.126
1.6	0.0474	0.0450	0.0221	0.0244	0.101	0.101

TABLE 3. COMPARISON OF EXACT AND APPROXIMATE VALUES OF $A(c)$, $p(c)$ AND $\rho(c)$ FOR A GAS WITH AN ISENTROPIC EXPONENT $\gamma = 1$

ρ varies in the range $0.1\rho_0 \leqslant \rho \leqslant \rho_0$ and approximate values correspond to $A = 0.4143A_0 \tan^2 (0.99886 - 0.24087c/A_0)$.

c/A_0	A_E/A_0	A/A_0	p_E/p_0	p/p_0	ρ_E/ρ_0	ρ/ρ_0
0.0	1.000	1.000	1.000	1.000	1.000	1.000
0.1	0.905	0.901	0.905	0.905	0.905	0.905
0.2	0.819	0.813	0.819	0.819	0.819	0.818
0.3	0.741	0.734	0.741	0.742	0.741	0.740
0.4	0.670	0.665	0.670	0.672	0.670	0.669
0.5	0.607	0.602	0.607	0.609	0.607	0.605
0.6	0.549	0.546	0.549	0.552	0.549	0.547
0.7	0.497	0.496	0.497	0.500	0.497	0.495
0.8	0.449	0.450	0.449	0.452	0.449	0.448
0.9	0.407	0.409	0.407	0.409	0.407	0.406
1.0	0.368	0.371	0.368	0.370	0.368	0.367
1.1	0.333	0.337	0.333	0.335	0.333	0.333
1.2	0.301	0.306	0.301	0.303	0.301	0.302
1.3	0.273	0.277	0.273	0.274	0.273	0.273
1.4	0.247	0.251	0.247	0.247	0.247	0.248
1.5	0.223	0.227	0.223	0.223	0.223	0.224
1.6	0.202	0.205	0.202	0.202	0.202	0.203
1.7	0.183	0.185	0.183	0.182	0.183	0.184
1.8	0.165	0.167	0.165	0.165	0.165	0.167
1.9	0.150	0.150	0.150	0.149	0.150	0.151
2.0	0.135	0.134	0.135	0.135	0.135	0.136
2.1	0.122	0.120	0.122	0.122	0.122	0.123
2.2	0.111	0.106	0.111	0.111	0.111	0.111
2.3	0.100	0.0942	0.100	0.101	0.100	0.100

PHILOSOPHICAL TRANSACTIONS OF THE ROYAL SOCIETY A MATHEMATICAL, PHYSICAL & ENGINEERING SCIENCES

With these values $\mu = 0.6856A_0^{-\frac{1}{2}}$ and $\nu = -0.8484A_0^{-\frac{3}{2}}$. (8.17)

The approximate values of $A(c)$, $p(c)$ and $\rho(c)$ are compared with their exact values in table 2. Again the maximum error is about $1\frac{1}{2}$ %.

The upper limit of γ for a gas is $\frac{5}{3}$, the lower limit is 1.0. For comparison, in table 3 the approximate values of $A(c)$, $p(c)$ and $\rho(c)$ are compared with their exact values given by

$$\frac{A_E}{A_0} = \frac{p_E}{p_0} = \frac{\rho_E}{\rho_0} = e^{-c/A_0}.$$

The approximate values correspond to

$$\theta_0 = 0.9989, \quad \theta_1 = -0.2409, \quad \theta_2 = 0.4143,$$

while $t_0 = 2.6724$ and $e_0 = -6.4496$.

With these values $\mu = -0.3101A_0^{-\frac{1}{2}}$ and $\nu = -0.7484A_0^{-\frac{3}{2}}$.

The maximum error is again about $1\frac{1}{2}$ %. The values of the parameters have been determined by the method of least squares.

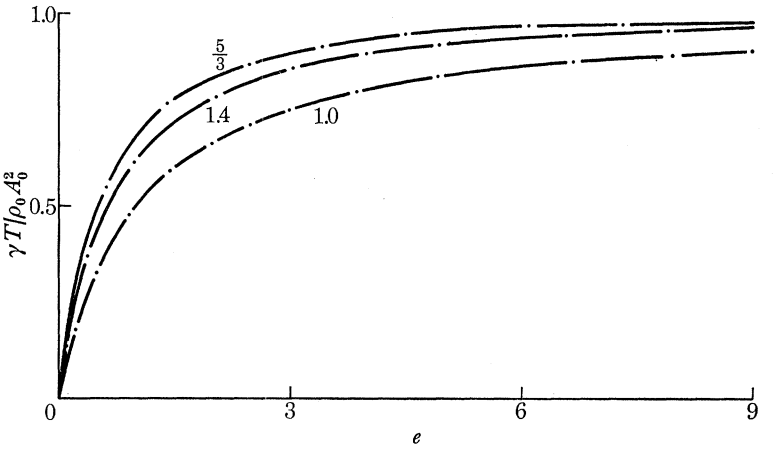

FIGURE 6. Comparison of the exact stress–strain relations for gases with isentropic exponents $\gamma = 1$, 1.4 and $\frac{5}{3}$ with model stress–strain relations. The strain e varies over the range $0 \leqslant e \leqslant 9$ which corresponds to a density variation $0.1\rho_0 \leqslant \rho \leqslant \rho_0$. ———, Model equation; . . . . . , $p/p_0 = (\rho/\rho_0)^\gamma$.

Gases are examples of elastic materials which soften in extension in the sense that as the strain e increases the Lagrangian sound speed A decreases monotonically to zero. For later reference, in figure 6 we have depicted the variations of T with e when $\gamma = 1.0$, 1.4 and $\frac{5}{3}$. The exact and approximate curves are not distinguishable.

It should be noted that equations (8.7) to (8.11) with the parameters given by equations (8.14) to (8.17) cannot be used to approximate the behaviour of a gas in the limit as $\rho/\rho_0 \to 0$. In this limit the exact law (8.3) must be used. For example, equations (8.7) and (8.16) predict that when $\gamma = 1.4$ the limiting value of c/A_0 is 2.75: actually, the exact limiting value is 5.0. The above relations, which provide an excellent curve fit for $0.1\rho_0 \leqslant \rho \leqslant \rho_0$, cannot also be used to provide a good fit in the range $0 \leqslant \rho \leqslant 0.1\rho_0$.

Bell (1968) has shown that during dynamic uniaxial compression many polycrystalline solids obey a stress–strain law which, away from $e_E = 0$, can be curve fitted by the simple parabolic law

$$\frac{T_E}{T_M} = \left(\frac{e_E}{e_M}\right)^{\frac{1}{2}}. \tag{8.18}$$

In equation (8.18), $T_M\,(<0)$ and $e_M\,(<0)$ are any two values of stress and strain which occur simultaneously. In what follows we take $-e_M$ as the maximum compressive strain which occurs during the deformation and $-T_M$ to be the maximum compressive stress. The law (8.18) only holds at a particle during compression. If

$$A_M = \left(\frac{1}{2\rho_0}\frac{T_M}{e_M}\right)^{\frac{1}{2}} \quad \text{and} \quad c_M = \tfrac{4}{3}e_M A_M \tag{8.19}$$

denote the values of A and $c\,(<0)$ when $(T_E, e_E) = (T_M, e_M)$ then, when (8.18) holds,

$$\frac{A_E}{A_M} = \left(\frac{c}{c_M}\right)^{-\frac{1}{3}}, \quad \frac{e_E}{e_M} = \left(\frac{c}{c_M}\right)^{\frac{4}{3}}, \quad \text{and} \quad \frac{T_E}{T_M} = \left(\frac{c}{c_M}\right)^{\frac{2}{3}}. \tag{8.20}$$

Even when $A_E(c)$ is given by the simple expression (8.20) the hodograph equation (7.31) cannot be integrated. However, to the same approximation that the experimental data can be curve fitted by the laws (8.20) it can also be fitted by one of the model equations of state for which the hodograph equation can be integrated. This equation of state does not belong to the same family as that used to curve fit the response of a gas. It belongs to the other family of solutions to equations (7.6) and (8.9) for which

$$\frac{A}{A_0} = \eta_2 \coth^2\left(\eta_0 + \eta_1 \frac{c}{A_0}\right), \tag{8.21}$$

where
$$A_0^{\frac{1}{2}}\mu = 2\eta_1\eta_2^{\frac{1}{2}} \quad \text{and} \quad A_0^{\frac{3}{2}}\nu = 2\eta_1\eta_2^{-\frac{1}{2}}. \tag{8.22}$$

Then,
$$\frac{T}{\rho_0 A_0^2} = t_0 + \eta_2\eta_1^{-1}\left[\eta_1\frac{c}{A_0} - \coth\left(\eta_0 + \eta_1\frac{c}{A_0}\right)\right] \tag{8.23}$$

and
$$e = e_0 + (\eta_1\eta_2)^{-1}\left[\eta_1\frac{c}{A_0} - \tanh\left(\eta_0 + \eta_1\frac{c}{A_0}\right)\right]. \tag{8.24}$$

When conditions (8.13) hold

$$\eta_2 = \tanh^2\eta_0, \quad t_0 = \eta_1^{-1}\tanh\eta_0 \quad \text{and} \quad e_0 = \eta^{-1}\coth\eta_0. \tag{8.25}$$

The laws (8.20) are not valid in some neighbourhood of $c = 0$. In practice, typically, they hold when c/c_M varies in the range

$$0.1 \leqslant \frac{c}{c_M} \leqslant 1, \quad \text{which corresponds to} \quad 0.046 \leqslant \frac{e_E}{e_M} \leqslant 1. \tag{8.26}$$

When $-e_M = 4\times10^{-2}$, which is a typical maximum compressive strain considered by Bell, this corresponds to e_E varying over the range $1.8\times10^{-3} \leqslant -e_E \leqslant 4\times10^{-2}$.

Since Bell's law predicts that A_0, the Lagrangian speed in the reference state, is unbounded, it is best to consider A/A_M, T/T_M and e/e_M as functions of c/c_M. Then, an excellent fit to Bell's laws over the range (8.26) is obtained from the model equations

$$\frac{A}{A_M} = 0.9655\coth^2\left(0.6785 + 1.4088\frac{c}{c_M}\right), \tag{8.27}$$

$$\frac{T}{T_M} = 0.8274 + 0.6437\frac{c}{c_M} - 0.4569\coth\left(0.6785 + 1.4088\frac{c}{c_M}\right), \tag{8.28}$$

$$\frac{e}{e_M} = 0.5693 + 1.3809\frac{c}{c_M} - 0.9802\tanh\left(0.6785 + 1.4088\frac{c}{c_M}\right). \tag{8.29}$$

If Bell's parabolic law is written
$$-T = 2\rho_0\gamma^2(-e)^{\frac{1}{2}}, \tag{8.30}$$

where γ is a material constant, then

$$T_{\mathrm{M}} = -2\rho_0\gamma^2|e_{\mathrm{M}}|^{\frac{1}{2}}, \quad A_{\mathrm{M}} = \gamma|e_{\mathrm{M}}|^{-\frac{1}{4}} \quad \text{and} \quad c_{\mathrm{M}} = -\tfrac{4}{3}\gamma|e_{\mathrm{M}}|^{\frac{3}{4}}, \tag{8.31}$$

while in equation (7.6)

$$\beta^{\frac{1}{2}}\mu = -2.0765|e_{\mathrm{M}}|^{-\frac{7}{8}} \quad \text{and} \quad \beta^{\frac{3}{2}}\nu = 2.1506|e_{\mathrm{M}}|^{-\frac{5}{8}}.$$

TABLE 4. COMPARISON OF THE VALUES OF $A(c)$, $T(c)$ AND $e(c)$ PREDICTED BY BELL'S PARABOLIC EQUATION OF STATE, FOR WHICH $A_{\mathrm{E}}/A_{\mathrm{M}} = (c/c_{\mathrm{M}})^{-\frac{1}{3}}$, WITH A MODEL EQUATION OF STATE FOR WHICH $A = 0.96554A_{\mathrm{M}}\coth^2(0.67845 + 1.4088\, c/c_{\mathrm{M}})$

The parameters have been chosen to obtain a best fit as c varies in the range $0.1c_{\mathrm{M}} \leqslant c \leqslant c_{\mathrm{M}}$.

c/c_{M}	$A_{\mathrm{E}}/A_{\mathrm{M}}$	A/A_{M}	$T_{\mathrm{E}}/T_{\mathrm{M}}$	T/T_{M}	$e_{\mathrm{E}}/e_{\mathrm{M}}$	e/e_{M}
0.1	2.154	2.121	0.215	0.215	0.046	0.046
0.2	1.710	1.743	0.342	0.342	0.117	0.116
0.3	1.494	1.505	0.448	0.450	0.201	0.199
0.4	1.357	1.349	0.543	0.545	0.295	0.292
0.5	1.260	1.242	0.630	0.631	0.397	0.396
0.6	1.186	1.168	0.711	0.711	0.506	0.506
0.7	1.126	1.114	0.788	0.787	0.622	0.624
0.8	1.077	1.076	0.862	0.860	0.743	0.745
0.9	1.036	1.048	0.932	0.931	0.869	0.871
1.0	1.000	1.027	1.000	1.000	1.000	1.000

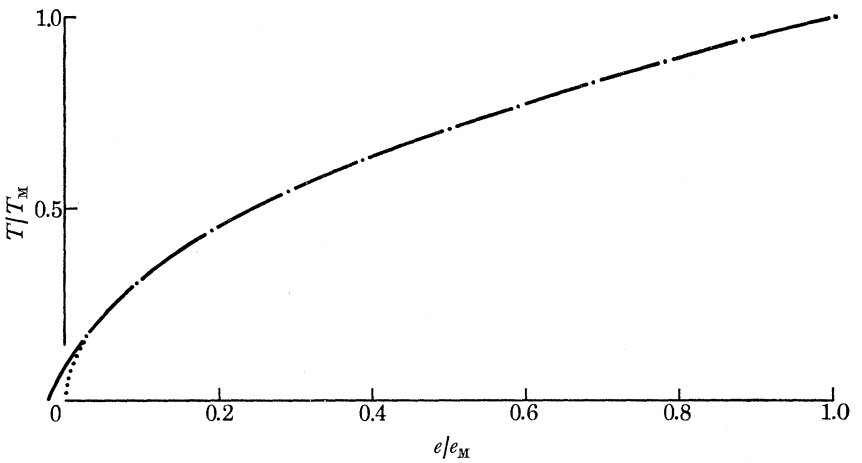

FIGURE 7. Comparison of Bell's parabolic stress–strain relation with a model stress–strain relation. ———, Model equation; . . . . . , Bell's parabolic law.

Table 4 compares the values of A_{E}, T_{E} and e_{E} given by equations (8.20) with the values of A, T and e given by equations (8.27) to (8.29) when c varies in the range $0.1c_{\mathrm{M}} \leqslant c \leqslant c_{\mathrm{M}}$. The maximum error in T and e is around $\frac{1}{3}$ %! The maximum error in A is 3 %. In figure 7 the model stress–strain curve is compared with Bell's parabolic curve as c varies over the full range

$$0 \leqslant c \leqslant c_{\mathrm{M}}.$$

They are not distinguishable as e varies over 97 % of its range.

8.3. *General classification of material responses*

Figures 8 to 11 illustrate the various material responses which can be modelled by an appropriate choice of the parameters ν, μ and A_0. Figure 8 illustrates the typical behaviour of a *soft*

elastic material, or, more strictly, of a material which softens relative to its reference state. For a material, such as aluminum, which softens in tension the Lagrangian sound speed A decreases monotonically from its value A_0 at $e = 0$ to some non-zero asymptotic value A_∞ as e increases. Other materials, such as the polycrystalline solids studied by Bell, soften in compression. For these materials, the condition that $\rho > 0$ implies that e can only vary in the range $-1 < e \leqslant 0$ so that the actual limiting value A_∞ cannot be attained. However, over this range of strain the smallest value of A need not be significantly different from A_∞. Once the parameters A_0 and A_∞ have been specified there still remains one other parameter which can also be specified.

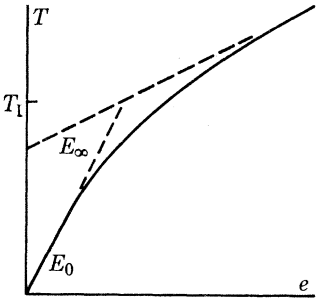

FIGURE 8

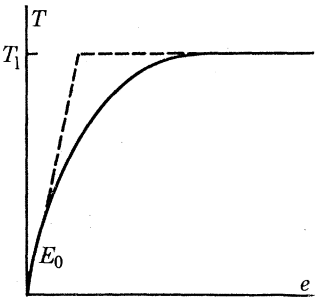

FIGURE 9

FIGURE 8. A typical stress–strain relation for a soft elastic material. The sound speed A decreases monotonically with either increasing or decreasing e from $A_0 = \sqrt{(E_0/\rho_0)}$ at $e = 0$ to some limiting value $A_\infty = \sqrt{(E_\infty/\rho_0)}$. The values of E_0, E_∞ and T_1 can be specified.

FIGURE 9. A typical stress–strain relation for an ideally soft elastic material. The sound speed A decreases monotonically with either increasing or decreasing e from $A_0 = \sqrt{(E_0/\rho_0)}$ at $e = 0$ to zero. The values of E_0, the limiting stress T_1, and the value of e at which $T = 0.99T_1$ can be specified.

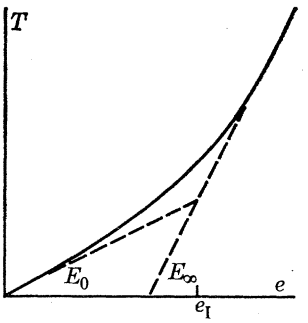

FIGURE 10

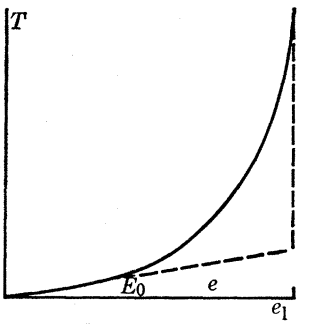

FIGURE 11

FIGURE 10. A typical stress–strain relation for a hard elastic material. The sound speed A increases monotonically with either increasing or decreasing e from $A_0 = \sqrt{(E_0/\rho_0)}$ at $e = 0$ to some limiting value $A_\infty = \sqrt{(E_\infty/\rho_0)}$. The values of E_0, E_∞ and e_I can be specified.

FIGURE 11. A typical stress–strain relation for an ideally hard elastic material. The sound speed A increases monotonically without bound with either increasing or decreasing e. The values of E_0, the limiting strain e_1, and the value of T at which $e = 0.99e_1$ can be specified.

This can be chosen to control the rate at which A varies with e between its two limiting values A_0 and A_∞. One good measure of this is the value of e, $= e_I$ say, at which the tangents to the stress–strain curve at $e = 0$ and $|e| = \infty$ intersect. At this point $(T, e) = (\rho_0 A_0^2 e_I, e_I)$. For materials which soften in extension $e_I > 0$, for materials which soften in compression $e_I < 0$.

When, for all practical purposes, $A_\infty = 0$, as it is for a gas during expansion, the medium is called *ideally soft*. Then, for materials which soften in extension, no matter how large e the traction T can never exceed a limiting value T_1. Similarly, for materials which soften in compression, no matter how large $-e$, $-T$ can never exceed $-T_1$. (For a gas $T_1 = p_0$, the pressure

in the reference state.) Once A_0 and T_1 have been specified the other parameter can be chosen to control the rate at which the asymptotic value, T_1, of T is approached. One of the many ways to do this is to specify the value of e at which $T = 0.99T_1$.

Figure 10 illustrates the behaviour of a *hard* elastic material. As either e, or $-e$, increases A increases monotonically from A_0 to some finite limiting value A_∞. Collagen tissue and vulcanized rubbers are examples of materials which harden in extension, foams and soils are examples of materials which harden in compression. Again, in addition to A_0 and A_∞, e_I can be specified. Finally, figure 11 depicts the behaviour of an *ideally hard* elastic material. Here, if the material is ideally hard in tension, no matter how large T, e can never exceed some limiting value e_1. Similarly, if the material is ideally hard in compression, no matter how large $-T$, $-e$ can never exceed some limiting value $-e_1$. In addition to A_0 and e_1, the value of T at which $e = 0.99e_1$ can also be specified.

Of course the prescription given above of how to choose the parameters A_0, μ and ν is somewhat arbitrary. In practice, other choices might be more appropriate. The aim has been to show that the model equations of state can approximate the basic features of the reponses depicted in figures 7 to 10.

8.4 *Correlation of stress–strain curves*

(i) *Non-ideal materials*

The three parameter family of stress–strain curves describing the responses of non-ideal materials can be correlated by a one parameter family of curves by simply plotting T/T_I against e/e_I. Any curve in this family is uniquely determined once the parameter

$$M = -\frac{\mu}{\nu A_0} = \frac{A_\infty}{A_0} \ (> 0) \tag{8.32}$$

has been specified. Materials which soften correspond to M varying in the range $0 \leqslant M < 1$, those which harden correspond to M varying in the range $1 < M \leqslant \infty$. The special case $M = 1$ corresponds to a material which obeys Hooke's law. This follows from the fact that equations (7.6) and (8.9) have solutions which can be written

$$\frac{T}{T_I} = (1+M)\left[1+M^{\frac{1}{2}}\left(\bar{c}-\frac{1+M^{\frac{1}{2}}\tanh\bar{c}}{M^{\frac{1}{2}}+\tanh\bar{c}}\right)\right], \tag{8.33}$$

$$\frac{e}{e_I} = (1+M^{-1})\left[1+M^{-\frac{1}{2}}\left(\bar{c}-\frac{M^{\frac{1}{2}}+\tanh\bar{c}}{1+M^{\frac{1}{2}}\tanh\bar{c}}\right)\right] \tag{8.34}$$

and

$$\frac{A}{A_0} = M\left(\frac{1+M^{\frac{1}{2}}\tanh\bar{c}}{M^{\frac{1}{2}}+\tanh\bar{c}}\right)^2, \tag{8.35}$$

where

$$\bar{c} = \frac{M^{\frac{1}{2}}}{1+M}\frac{c}{e_I A_0}. \tag{8.36}$$

In terms of A_0, A_∞ and e_I

$$\mu = \frac{2A_\infty}{A_0+A_\infty}\frac{A_0^{-\frac{1}{2}}}{e_I}, \quad \nu = -\frac{2}{A_0+A_\infty}\frac{A_0^{-\frac{1}{2}}}{e_I} \quad \text{and} \quad T_I = \rho_0 A_0^2 e_I. \tag{8.37}$$

The family of stress–strain curves described by equations (8.21) to (8.25) are identical to those described by equations (8.33) to (8.36) when $0 \leqslant M \leqslant 1$. The equivalence is easily verified by putting

$$M = \tanh^2\eta_0 \quad \text{and} \quad e_I = \frac{\tanh\eta_0}{1+\tanh^2\eta_0}\eta_1^{-1} \tag{8.38}$$

in these latter equations.

PHILOSOPHICAL TRANSACTIONS OF THE ROYAL SOCIETY A MATHEMATICAL, PHYSICAL & ENGINEERING SCIENCES

In the limit as $M \to 0$ equations (8.33) to (8.37) imply that

$$\frac{T}{T_I} = 1 - \left(1 + \frac{c}{A_0 e_I}\right)^{-1}, \quad \frac{e}{e_I} = \frac{1}{3}\left[\left(1 + \frac{c}{A_0 e_I}\right)^3 - 1\right] \tag{8.39}$$

and

$$\frac{A}{A_0} = \left(1 + \frac{c}{A_0 e_I}\right)^{-2}, \quad \text{while} \quad \mu = 0 \quad \text{and} \quad \nu = -2 e_I^{-1} A_0^{-\frac{3}{2}}. \tag{8.40}$$

According to equations (8.39), when $M = 0$,

$$\frac{T}{T_I} = 1 - \left(1 + 3\frac{e}{e_I}\right)^{-\frac{1}{3}}. \tag{8.41}$$

In the limit as $M \to \infty$,

$$\frac{T}{T_I} = \frac{1}{3}\left[\left(1 + \frac{c}{A_0 e_I}\right)^3 - 1\right], \quad \frac{e}{e_I} = 1 - \left(1 + \frac{c}{A_0 e_I}\right)^{-1} \tag{8.42}$$

and

$$\frac{A}{A_0} = \left(1 + \frac{c}{A_0 e_I}\right), \quad \text{while} \quad \mu = 2 e_I^{-1} A_0^{-\frac{1}{2}} \quad \text{and} \quad \nu = 0. \tag{8.43}$$

According to equations (8.42), when $M = \infty$,

$$\frac{T}{T_I} = \frac{1}{3}\left[\left(1 - \frac{e}{e_I}\right)^{-3} - 1\right]. \tag{8.44}$$

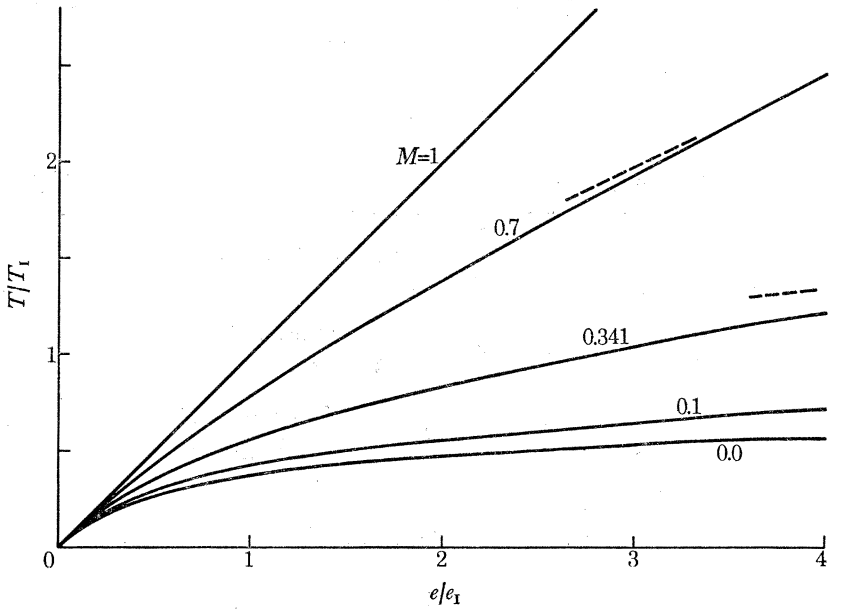

FIGURE 12. Typical variations of T/T_I with e/e_I for soft elastic materials. The parameter $M = A_\infty/A_0$. The case $M = 0.341$ corresponds to materials which satisfy Bell's parabolic law.

The non-ideal responses are described by equations (8.33) to (8.37) as $\bar{c}$ varies in the range $0 \leqslant \bar{c} \leqslant \infty$. $\bar{c}$ remains positive because if the material behaves non-ideally in extension both c and e_I are positive, while if it behaves non-ideally in compression both c and e_I are negative. In figures 12 and 13 the relations between T/T_I and e/e_I, which are described by these equations, have been plotted for typical values of the parameter M. Figure 11 exhibits curves which describe the behaviour of soft materials. These curves are bound by the curve $M = 0$, which corresponds to the law (8.41), and the curve $M = 1$ which corresponds to Hooke's law $T/T_I = e/e_I$.

The curve which corresponds to $M = 0.341$ has been included because part of it was used to curve fit Bell's parabolic law. Figure 12 exhibits curves which describe the behaviour of hard materials. They are bound by the curve $M = 1$ and the curve $M = \infty$ which corresponds to the law (8.44).

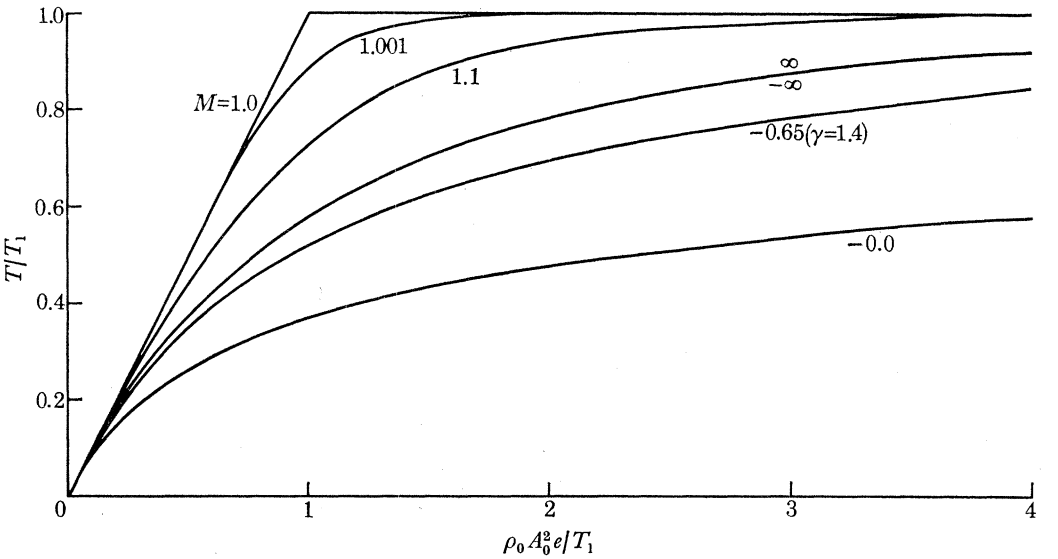

FIGURE 13. Typical variations of T/T_1 with $\rho_0 A_0^2 e/T_1$ for ideally soft elastic materials. The case $M = -0.65$ corresponds to a gas with isentropic exponent $\gamma = 1.4$.

(ii) *Ideally soft materials*

There are two families of curves which describe ideally soft materials. The first family is described by equations (8.33) to (8.37) as M and $\bar{c}$ vary in the ranges

$$1 \leqslant M \leqslant \infty \quad \text{and} \quad -\bar{\eta}_0 \leqslant \bar{c} \leqslant 0 \quad \text{where} \quad \coth \bar{\eta}_0 = M^{\frac{1}{2}}. \tag{8.45}$$

This is best seen by noting that these equations can be written

$$T/T_1 = (\bar{\eta}_0 - \tanh \bar{\eta}_0)^{-1}[\tanh(\bar{\eta}_0 + \bar{c}) - \bar{c} - \tanh \bar{\eta}_0], \tag{8.46}$$

$$\rho_0 A_0^2 e/T_1 = \tanh^4 \bar{\eta}_0 (\bar{\eta}_0 - \tanh \bar{\eta}_0)^{-1}[\coth(\bar{\eta}_0 + \bar{c}) - \bar{c} - \coth \bar{\eta}_0] \tag{8.47}$$

and

$$A/A_0 = \coth^2 \bar{\eta}_0 \tanh^2(\bar{\eta}_0 + \bar{c}), \tag{8.48}$$

where

$$\bar{c} = -\coth^2 \bar{\eta}_0 (\bar{\eta}_0 - \tanh \bar{\eta}_0)\, \rho_0 A_0 c/T_1. \tag{8.49}$$

In terms of A_0, the limiting stress T_1, and the parameter $\bar{\eta}_0$

$$\left.\begin{aligned} \mu &= -2 \coth^3 \bar{\eta}_0 (\bar{\eta}_0 - \tanh \bar{\eta}_0)\, \rho_0 A_0^{\frac{3}{2}}/T_1 \\ \text{and} \quad \nu &= 2 \coth \bar{\eta}_0 (\bar{\eta}_0 - \tanh \bar{\eta}_0)\, \rho_0 A_0^{\frac{1}{2}}/T_1. \end{aligned}\right\} \tag{8.50}$$

Note that, according to equations (8.46) to (8.48),

$$\text{as} \quad \bar{c} \to -\bar{\eta}_0, \quad \frac{T}{T_1} \to 1, \quad \frac{\rho_0 A_0^2}{T_1} e \to \infty \quad \text{and} \quad \frac{A}{A_0} \to 0. \tag{8.51}$$

Unlike the parameters T_1 and A_0 the parameter $\bar{\eta}_0$ in the above equations has no immediate physical interpretation. It can be chosen so that the model equation of state also approximates some other desired feature of the experimental curve. For example, $\bar{\eta}_0$ can be chosen so that

when $T = 0\ 99T_1$, $\rho_0 A_0^2 e/T_1$ has some specified value, ϵ say. The function $\overline{\eta}_0(\epsilon)$ can readily be determined numerically from equations (8.46) to (8.47). It, together with the functions $\mu(\epsilon)$ and $\nu(\epsilon)$, is plotted in figure 16. Several of the curves of the family described by equations (8.46) to (8.49) are drawn in figure 14. They are parameterized by

$$M = -\mu/A_0\nu = \coth^2\overline{\eta}_0. \tag{8.52}$$

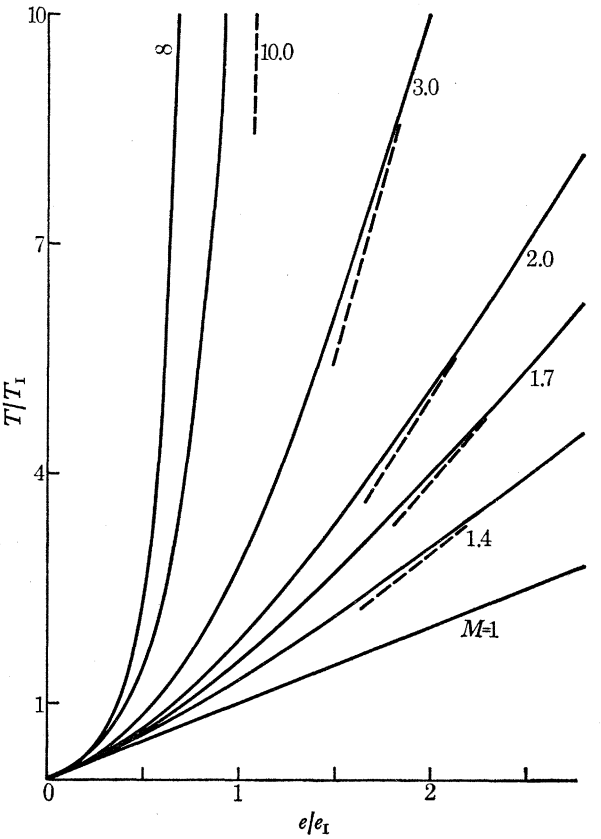

FIGURE 14. Typical variations of T/T_1 with e/e_1 for hard elastic materials. The parameter $M = A_\infty/A_0$.

Of special interest is the limit as $M \to 1$ ($\overline{\eta}_0 \to \infty$). Then, the usual linear elastic, perfectly soft response is obtained. According to equations (8.46) to (8.49), in the limit as $\overline{\eta}_0 \to \infty$, the dominant behaviour is described by the equations

$$\frac{\rho_0 A_0}{T_1} c = \frac{T}{T_1}, \quad \frac{\rho_0 A_0^2}{T_1} e = \frac{T}{T_1} + \overline{\eta}_0^{-1} \coth\left(\overline{\eta}_0\left[1 - \frac{T}{T_1}\right]\right) \tag{8.53}$$

and

$$\frac{A}{A_0} = \tanh^2\left(\overline{\eta}_0\left[1 - \frac{T}{T_1}\right]\right). \tag{8.54}$$

$A(c)$ given by equations (8.53) and (8.54) satisfies equation (7.6) with

$$\mu = -2\overline{\eta}_0 \frac{\rho_0 A_0^{\frac{3}{2}}}{T_1} \quad \text{and} \quad \nu = 2\overline{\eta}_0 \frac{\rho_0 A_0^{\frac{1}{2}}}{T_1}. \tag{8.55}$$

In the other limit as $M \to \infty$ ($\overline{\eta}_0 \to 0$)

$$\frac{T}{T_1} = 1 - \left(1 - \frac{1}{3}\frac{\rho_0 A_0}{T_1} c\right)^3, \quad \frac{\rho_0 A_0^2}{T_1} e = 3\left[\left(1 - \frac{1}{3}\frac{\rho_0 A_0}{T_1} c\right)^{-1} - 1\right] \tag{8.56}$$

and

$$\frac{A}{A_0} = \left(1 - \frac{1}{3}\frac{\rho_0 A_0}{T_1} c\right)^2 \quad \text{while} \quad \mu = -\frac{2}{3}\frac{\rho_0 A_0^{\frac{3}{2}}}{T_1} \quad \text{and} \quad \nu = 0. \tag{8.57}$$

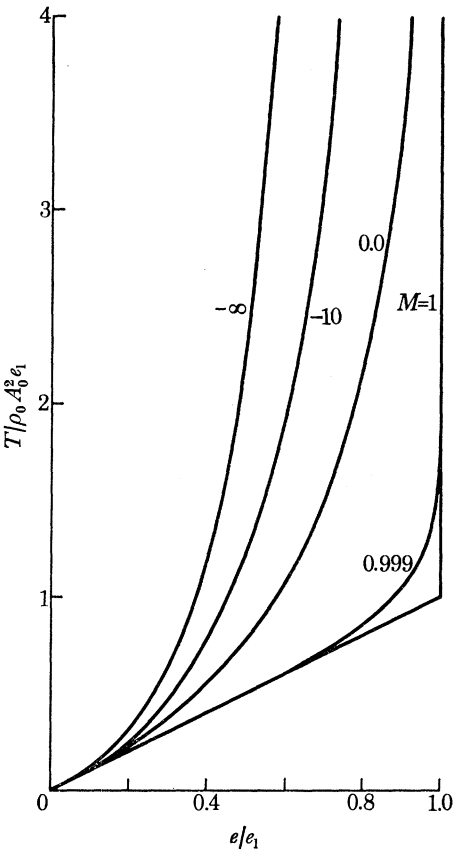

FIGURE 15. Typical variations of $T/\rho_0 A_0^2 e_1$ with e/e_1 for ideally hard elastic materials.

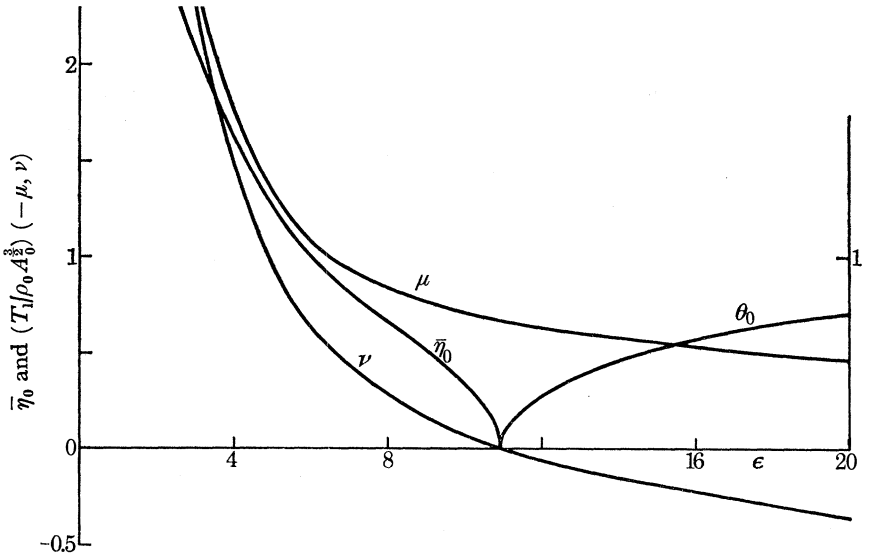

FIGURE 16. The variations of μ, ν, $\bar{\eta}_0$ and θ_0 with ϵ, the value of $\rho_0 A_0^2 e/T_1$ at which $T = 0.99 T_1$, for an ideally soft material. The variations of μ, ν, η_0 and $\bar{\theta}_0$ with τ, the value of $T/\rho_0 A_0^2 e_1$ at which $e = 0.99 e_1$, are obtained by replacing ϵ by τ, $(T_1/\rho_0 A_0^{\frac{3}{2}})\ (-\mu, \nu)$ by $e_1 A_0^{\frac{1}{2}}(\nu, -\mu)$, $\bar{\eta}_0$ by η_0 and θ_0 by $\bar{\theta}_0$.

If c is eliminated from equations (8.56) they yield the explicit stress–strain law

$$\frac{T}{T_1} = 1 - \left(1 + \frac{\rho_0 A_0^2}{3T_1} e\right)^{-3}. \tag{8.58}$$

According to figure 16 as $\overline{\eta}_0$ decreases in the range $[\infty, 0]$ ϵ increases from 0 to a maximum value of 10.9. If it is specified that $\rho_0 A_0^2 e/T_1 > 10.9$ when $T = 0.99T_1$ the family of curves described by equations (8.46) to (8.49) cannot be used. However, the family of curves described by equations (8.7) to (8.12) can. If we introduce the variable

$$\bar{c} = -\cot^2\theta_0[\tan\theta_0 - \theta_0]\frac{\rho_0 A_0}{T_1} c \left(= \frac{\theta_1}{A_0} c\right), \tag{8.59}$$

where the parameter θ_0 can take any value in the range $0 \leqslant \theta_0 \leqslant \frac{1}{2}\pi$, these equations can be written

$$T/T_1 = (\tan\theta_0 - \theta_0)^{-1}[\bar{c} - \tan(\theta_0 + \bar{c}) + \tan\theta_0], \tag{8.60}$$

$$\rho_0 A_0^2 e/T_1 = \tan^4\theta_0 (\tan\theta_0 - \theta_0)^{-1}[\cot(\theta_0 + \bar{c}) + \bar{c} - \cot\theta_0] \tag{8.61}$$

and

$$A/A_0 = \cot^2\theta_0 \tan^2(\theta_0 + \bar{c}). \tag{8.62}$$

In these equations $\bar{c}$ varies in the range $-\theta_0 \leqslant \bar{c} \leqslant 0$. The parameter

$$\left.\begin{aligned} \mu &= -2\cot^3\theta_0 (\tan\theta_0 - \theta_0)\rho_0 A_0^{\frac{3}{2}}/T_1, \\ \text{while} \quad \nu &= -2\cot\theta_0 (\tan\theta_0 - \theta_0)\rho_0 A_0^{\frac{1}{2}}/T_1. \end{aligned}\right\} \tag{8.63}$$

Several stress–strain curves belonging to the family of ideally soft materials which are described by equations (8.59) to (8.62) are also drawn in figure 14. These curves are again parametrized by

$$M = -\mu/A_0\nu = -\cot^2\theta_0, \tag{8.64}$$

which varies in the range $-\infty \leqslant M \leqslant 0$. The curve corresponding to $M = -0.65$ has been included since this was used to curve fit the stress–strain curve of a polytropic gas with $\gamma = 1.4$. In figure 16 the variations of $\theta_0(\epsilon)$, $\mu(\epsilon)$ and $\nu(\epsilon)$ as ϵ varies over the range $10.9 \leqslant \epsilon < \infty$ are also drawn.

In the limit as $M \to -\infty$ equations (8.59) to (8.63) are identical with equations (8.56) to (8.58). In the limit as $M \to 0$ they are identical with equations (8.41) to (8.44) with $T_I = T_1$ and

$$e_I = T_1/\rho_0 A_0^2.$$

(iii) *Ideally hard materials*

As for the ideally soft materials there are two families of curves which describe ideally hard materials. The first family is described by equations (8.33) to (8.37) as M and $\bar{c}$ vary in the ranges

$$0 \leqslant M \leqslant 1 \quad \text{and} \quad -\eta_0 \leqslant \bar{c} \leqslant 0 \quad \text{where} \quad \tanh\eta_0 = M^{\frac{1}{2}}. \tag{8.65}$$

Over these ranges equations (8.33) to (8.37) can be written in the form

$$T/\rho_0 A_0^2 e_1 = \tanh^4\eta_0(\eta_0 - \tanh\eta_0)^{-1}[\coth(\eta_0 + \bar{c}) - \bar{c} - \coth\eta_0], \tag{8.66}$$

$$e/e_1 = (\eta_0 - \tanh\eta_0)^{-1}[\tanh(\eta_0 + \bar{c}) - \bar{c} - \tanh\eta_0] \tag{8.67}$$

and

$$A/A_0 = \tanh^2\eta_0 \coth^2(\eta_0 + \bar{c}), \tag{8.68}$$

where

$$\bar{c} = -\coth^2\eta_0(\eta_0 - \tanh\eta_0)\, c/e_1 A_0 \quad (= \eta_1 c/A_0). \tag{8.69}$$

In terms of A_0, the limiting strain e_1, and the parameter η_0

$$\left.\begin{aligned}\mu &= -2\coth\eta_0(\eta_0-\tanh\eta_0)\,e_1^{-1}A_0^{-\frac{1}{2}}\\ \text{and}\quad \nu &= 2\coth^3\eta_0(\eta_0-\tanh\eta_0)\,e_1^{-1}A_0^{-\frac{3}{2}}.\end{aligned}\right\} \tag{8.70}$$

Again the parameter η_0 in the above equations has no direct physical interpretation. It can be chosen so that when $e = 0.99e_1$ the variable $T/\rho_0 A_0^2 e_1$ takes some prescribed value, τ say. The variations of η_0, μ and ν with τ are depicted in figure 16. Several of the curves of the family described by equations (8.66) to (8.70) are drawn in figure 14. They are parameterized by

$$M = -\mu/A_0\nu = \tanh^2\eta_0. \tag{8.71}$$

In the limit as $M\to 1$ ($\eta_0\to\infty$) the linear elastic, perfectly hard, response is obtained. According to equations (8.66) to (8.70), in the limit as $\eta_0\to\infty$, the dominant behaviour is described by the equations

$$c = A_0 e, \quad \frac{T}{\rho_0 A_0^2 e_1} = \frac{e}{e_1} + \eta_0^{-1}\coth\left(\eta_0\left[1-\frac{e}{e_1}\right]\right) \tag{8.72}$$

and

$$\frac{A}{A_0} = \coth^2\left(\eta_0\left[1-\frac{e}{e_1}\right]\right). \tag{8.73}$$

$A(c)$ given by equations (8.72) and (8.73) satisfies equation (7.6) with

$$\mu = -2\eta_0 e_1^{-1}A_0^{-\frac{1}{2}} \quad \text{and} \quad \nu = 2\eta_0 e_1^{-1}A_0^{-\frac{3}{2}}. \tag{8.74}$$

In the limit as $M\to 0$ ($\eta_0\to 0$)

$$\frac{T}{\rho_0 A_0^2 e_1} = 3\left[\left(1-\frac{1}{3}\frac{c}{A_0 e_1}\right)^{-1}-1\right], \quad \frac{e}{e_1} = 1-\left(1-\frac{1}{3}\frac{c}{e_1 A_0}\right)^3 \tag{8.75}$$

and

$$\frac{A}{A_0} = \left(1-\frac{1}{3}\frac{c}{A_0 e_1}\right)^{-2} \quad \text{while} \quad \mu = 0 \quad \text{and} \quad \nu = \tfrac{2}{3}e_1^{-1}A_0^{-\frac{3}{2}}. \tag{8.76}$$

If c is eliminated from equations (8.75) and (8.76) they yield the explicit stress–strain law

$$\frac{T}{\rho_0 A_0^2 e_1} = 3\left[\left(1-\frac{e}{e_1}\right)^{-\frac{1}{3}}-1\right]. \tag{8.77}$$

It was this relation which was used to correlate the responses of clays and saturated soils in §5.

The family of curves described by equations (8.66) to (8.70) can be used only when $\tau < 10.9$. When $\tau > 10.9$ the family of curves described by equations (8.7) to (8.12) must be used with $\bar\theta_0 = \theta_0 - \frac{1}{2}\pi$ and $\bar c = \theta_1 c/A_0$ varying over the ranges

$$0 \leqslant \bar\theta_0 \leqslant \tfrac{1}{2}\pi \quad \text{and} \quad -\bar\theta_0 \leqslant \bar c \leqslant 0. \tag{8.78}$$

In terms of e_1, $\bar\theta_0$ and $\bar c$ these equations can be written

$$T/\rho_0 A_0^2 e_1 = \tan^4\bar\theta_0(\tan\bar\theta_0-\bar\theta_0)^{-1}[\cot(\bar\theta_0+\bar c)+\bar c-\cot\bar\theta_0], \tag{8.79}$$

$$e/e_1 = (\tan\bar\theta_0-\bar\theta_0)^{-1}[\bar c-\tan(\bar\theta_0+\bar c)+\tan\bar\theta_0] \tag{8.80}$$

and

$$A/A_0 = \tan^2\bar\theta_0\cot^2(\bar\theta_0+\bar c), \tag{8.81}$$

where

$$\bar c = -\cot^2\bar\theta_0(\tan\bar\theta_0-\bar\theta_0)\,c/A_0 e_1. \tag{8.82}$$

The parameter

$$\left.\begin{aligned}\mu &= 2\cot\bar\theta_0(\tan\bar\theta_0-\bar\theta_0)\,e_1^{-1}A_0^{-\frac{1}{2}}\\ \text{and}\quad \nu &= 2\cot^3\bar\theta_0(\tan\bar\theta_0-\bar\theta_0)\,e_1^{-1}A_0^{-\frac{3}{2}}.\end{aligned}\right\} \tag{8.83}$$

Several stress–strain curves belonging to the class of ideally hard materials which are described by equations (8.79) to (8.83) are also drawn in figure 14. These curves are parameterized by

$$M = -\mu/A_0\nu = -\tan^2\bar{\theta}_0, \tag{8.84}$$

which varies in the range $-\infty \leqslant M \leqslant 0$. In figure 16 we have depicted the variations of $\bar{\theta}_0$, μ and ν with τ over the range $10.9 \leqslant \tau < \infty$.

In the limit as $M \to 0$ equations (8.79) to (8.83) are identical with equations (8.75) to (8.77). In the limit as $M \to \infty$ they are identical with equations (8.42) to (8.44) with $e_{\mathrm{I}} = e_1$ and

$$T_{\mathrm{I}} = \rho_0 A_0^2 e_1.$$

8.5. *Shear waves*

For shear waves the independent variable c in equation (7.6) must be replaced by $|c|$ and the coefficients of $F'(\alpha)$ and $G'(\beta)$ must be multiplied by $\operatorname{sgn} c$, the sign of c. Otherwise, the analysis follows that for stretching waves.

In practice, of course, it is not expected that the model equations of state will curve fit the experimental stress–strain curves of actual materials as closely as they do those for gases and for those polycrystalline solids which can be fitted by Bell's parabolic law. However, by a judicious choice of the free parameters in these model laws it should be possible to infer the broad features of the behaviour of many materials from the behaviour of the model materials in similar situations. Once the skeleton of the actual stress–strain relation has been approximated by one of the model laws the effect of its flesh can be approximated by using perturbation techniques which allow the parameters (μ, ν) in equation (7.6) to vary slowly with A.

9. Reflexion and transmission of a pulse at an interface

As a first illustration of the use of the model equations of state we show how to calculate the reflected and transmitted pulses which are generated when a pulse is incident at the free interface $X = 0$. We suppose that as the pulse passes $X = D$ it is a shockless simple wave for some time interval $0 \leqslant t \leqslant t_{\mathrm{R}}$. In this wave $F \equiv 0$ and at $X = D$ the signal function $G(t)$ $(= u = c)$ is known. For definiteness, this pulse can be thought of as that which is transmitted into the bounded medium when a pulse travelling through the semi-infinite medium to its right reaches the interface $X = D$. Alternatively, it can be thought of as the centred expansion wave which is generated in a shock tube when the diaphragm at $X = D$ bursts.

To calculate conditions at the interface $X = 0$ equation (7.15) is used. This equation is regarded as an ordinary differential equation governing the variation of t with β at any fixed X. Since G, and consequently A, are known functions of β $(= t)$ at $X = D$, for β varying in the range $[0, t_{\mathrm{R}}]$ the functions $G(\beta)$ and $n(\beta)$ $(= A^{\frac{1}{2}}$ at $X = D)$ which occur in this equation are known. As the pulse moves towards the interface $X = 0$ it remains a simple wave until it is affected by the reflected wave which is produced once its front $\beta = 0$ reaches $X = 0$. At all X in this simple wave $F \equiv 0$ and $A^{\frac{1}{2}} \equiv n(\beta)$. Then, equation (7.15) integrates to give the usual result

$$t = \beta + \frac{D - X}{A(G)} = \beta + \frac{D - X}{n^2(\beta)}. \tag{9.1}$$

To obtain the result (9.1) from equation (7.15) the fact that $A(c)$ satisfies equation (7.6) has been used. Condition (9.1) together with the conditions that in the simple wave

$$u = c = G(\beta) \tag{9.2}$$

are sufficient to calculate the variations of all the state variables with t at any X. As is typical for nonlinear problems, these variations are not given as explicit functions of t but parametrically in terms of the characteristic variable β.

Once the pulse enters the interaction region I_L neighbouring the interface $X = 0$ the signal function F is not identically zero. Consequently, the factor $A^{\frac{1}{2}}$ in equation (7.15), which will be referred to as the interaction term because it is the only term in this equation which is affected by the signal carried by the α-wave, is not, in general, a known function of (β, X). Accordingly, equation (7.15) cannot, by itself, be used to calculate the variations of t with β at all points of I_L. The important exception is at the free interface $X = 0$, where according to equations (4.8) and (4.14)

$$F = L(G) \quad \text{and} \quad c = G + L(G), \tag{9.3}$$

so that $A^{\frac{1}{2}}$ is a known function of β, $= \hat{m}(\beta)$ say. When this information is inserted, at $X = 0$ equation (7.15) reads

$$\hat{m}(\beta)\frac{\mathrm{d}}{\mathrm{d}\beta}\left(t - \beta + \frac{\nu}{\mu}D\right) + \mu\left(t - \beta + \frac{\nu}{\mu}D\right)G'(\beta) = n(\beta) - \hat{m}(\beta). \tag{9.4}$$

Once the linear first-order equation (9.4) has been solved subject to the initial condition that

$$\text{when} \quad \beta = 0, \quad t = D/A_0, \tag{9.5}$$

the variation of G with t at $X = 0$ is known Equation (9.3) then gives $F(t)$, the signal carried by the reflected wave, so that the variations of all the state variables at the interface can be calculated, as can the signal $G_L(t)$ $(= u$ at $X = 0)$ carried by the transmitted wave. The solution to equation (9.4) can, of course, be reduced to a simple quadrature which must, in general, be evaluated numerically.

9.1. *Reflexion of a centred wave*

As an illustration of the above results we consider the reflexion of a shockless centred simple wave from an interface. Such a wave is produced, and centred, at $X = D$ when A decreases discontinuously from A_0 to some value $< A_0$. In the shock-tube problem this occurs when the diaphragm bursts. It also occurs when the end of a string which is made of a material which softens in extension is suddenly pulled. A shockless centred wave also occurs when a bar which is made of a material which softens in compression is suddenly loaded at its end by a compressive force.

For waves which are centred at $X = D$ equation (7.15) must be interpreted rather carefully because at this singular point G changes by a finite amount over a vanishingly small variation in β $(= t$ at $X = D)$. The simplest way of deriving the limiting form of equation (7.15) is to consider the case when the incident simple wave is centred not at $X = D$ but at some point $X = X_0 < D$ at some time $t = t_0 > 0$, and then take the limit $(X_0, t_0) \to (D, 0)$. In such a centred wave

$$A = (X_0 - X)/(t - t_0). \tag{9.6}$$

According to equation (9.1) this implies that $G(\beta)$ is determined from the relation

$$A(G) = (X_0 - D)/(\beta - t_0). \tag{9.7}$$

When β, given in terms of G by equation (9.7), is inserted in equation (7.15) it yields the result that

$$\text{at any } X, \quad A^{\frac{1}{2}}(\mathrm{d}t/\mathrm{d}G) + [\mu(t - t_0) + \nu(X_0 - X)] = 0. \tag{9.8}$$

PHILOSOPHICAL TRANSACTIONS OF THE ROYAL SOCIETY A MATHEMATICAL, PHYSICAL & ENGINEERING SCIENCES

To obtain the important equation (9.8) the facts that $N(\beta) = A^{\frac{1}{2}}(G)$ and that $A(c)$ satisfies equation (7.6) have been used. The special values $(X_0, t_0) = (D, 0)$ do not introduce any singular behaviour in equation (9.8). As a check on this equation note that in the simple wave region where $G = c$ it integrates to give the result (9.6).

At the interface $X = 0$, where c is given in terms of G by equation (9.3), equation (9.8) predicts that G varies with t according to the simple law

$$A^{\frac{1}{2}}(\mathrm{d}t/\mathrm{d}G) + \mu t + \nu D = 0. \tag{9.9}$$

This equation integrates to give

$$\frac{A_0 t}{D} = 1 + \frac{1-M}{M}\left(1 - \exp\left[-\mu \int_0^G A^{-\frac{1}{2}} \mathrm{d}G\right]\right), \tag{9.10}$$

where $M = -\mu/A_0\nu$. The constant of integration in (9.10) has been determined from the condition that the front of the centred wave at which $G = 0$ arrives at $X = 0$ at $t = D/A_0$. Equation (9.1) determines the variation of G with t at the interface $X = 0$. Once this has been computed the variation of F with t follows from equation (9.3).

In what follows the variations of the state variables at the interface $X = 0$ are compared with their variations at any point X in the incident centred simple wave. These variations follow from the fact that in this incident wave

$$u = c \quad \text{and} \quad \frac{A_0 t}{D - X} = \frac{A_0}{A}. \tag{9.11}$$

For the non-ideal soft materials described by equations (8.32) to (8.37) equations (9.11) imply that

$$\frac{u}{A_0 e_{\mathrm{I}}} = \frac{1+M}{M^{\frac{1}{2}}}\bar{c}, \quad \text{where} \quad \frac{A_0 t}{D-X} = \left(\frac{1 + M^{-\frac{1}{2}}\tanh\bar{c}}{1 + M^{\frac{1}{2}}\tanh\bar{c}}\right)^2, \tag{9.12}$$

and where $M \leqslant 1$. For the class of ideal soft materials described by equations (8.45) to (8.50), equations (9.11) imply that

$$\left.\begin{aligned} \rho_0 A_0 u/T_{\mathrm{I}} &= -\tanh^2\bar{\eta}_0(\bar{\eta}_0 - \tanh\bar{\eta}_0)^{-1}\bar{c}, \\ \text{where} \qquad A_0 t/D - X &= \tanh^2\bar{\eta}_0 \coth^2(\bar{\eta}_0 + \bar{c}), \end{aligned}\right\} \tag{9.13}$$

while for the class of ideal soft materials described by equations (8.59) to (8.63)

$$\left.\begin{aligned} \rho_0 A_0 u/T_{\mathrm{I}} &= -\tan^2\theta_0(\tan\theta_0 - \theta_0)^{-1}\bar{c}, \\ \text{where} \qquad A_0 t/(D-X) &= \tan^2\theta_0 \cot^2(\theta_0 + \bar{c}). \end{aligned}\right\} \tag{9.14}$$

A centred simple wave cannot be generated in a Hookean material. This is because the Lagrangian sound speed A_0 does not vary with c so that any initial discontinuity which is produced in c cannot be smoothed by amplitude dispersion, but will propagate as a discontinuity. This limiting behaviour is described by equations (9.12) as $M \to 1$. To a first approximation

$$\frac{u}{A_0 e_{\mathrm{I}}} = -\ln\left[1 - \frac{1}{1-M}\left(\frac{A_0 t}{D-X} - 1\right)\right] \quad \text{as} \quad M \to 1-. \tag{9.15}$$

According to equation (9.15), as $M \to 1$, $u/A_0 e_{\mathrm{I}}$ changes by a finite amount in a layer neighbouring the front of the pulse where

$$\frac{A_0 t}{D-X} - 1 = O(1-M). \tag{9.16}$$

Certain other limiting cases of equations (9.12) to (9.14) deserve special mention. In the limit when $M \to 0$, (8.41) and equations (9.12) imply that in the incident wave

$$\frac{u}{A_0 e_{\mathrm{I}}} = \left(\frac{A_0 t}{D-X}\right)^{\frac{1}{2}} - 1 \quad (M = 0). \tag{9.17}$$

In the limit as $\bar{\eta}_0 \to 0$ the material response is described by equations (8.56) to (8.58) and equation (9.13) implies that

$$\frac{\rho_0 A_0}{T_1} u = 3\left[1 - \left(\frac{A_0 t}{D-X}\right)^{-\frac{1}{2}}\right] \quad (\bar{\eta}_0 = 0). \tag{9.18}$$

Finally, in the non-uniform limit as $\bar{\eta}_0 \to \infty$ the material response is described by equations (8.53) to (8.55) and equations (9.13) imply that u is determined from the relation

$$\frac{A_0 t}{D-X} = \tanh^2 \bar{\eta}_0 \coth^2\left[\bar{\eta}_0\left(1 - \frac{\rho_0 A_0}{T_1} u\right)\right] \quad \text{as} \quad \bar{\eta}_0 \to \infty. \tag{9.19}$$

According to this relation, $\rho_0 A_0 u/T_1$ can change from zero to any finite value < 1 in a layer neighbouring the wavefront where

$$\frac{A_0 t}{D-X} = 1 + O(\mathrm{e}^{-2\bar{\eta}_0}) \quad \text{as} \quad \bar{\eta}_0 \to \infty. \tag{9.20}$$

In this layer, to a first approximation, equation (9.19) predicts that

$$\frac{\rho_0 A_0}{T_1} u = (2\bar{\eta}_0)^{-1} \ln\left[1 + \tfrac{1}{4}\mathrm{e}^{2\bar{\eta}_0}\left(\frac{A_0 t}{D-X} - 1\right)\right]. \tag{9.21}$$

In a layer where

$$\bar{\eta}_0\left(1 - \frac{\rho_0 A_0}{T_1} u\right) = o(1) \quad \text{as} \quad \bar{\eta}_0 \to \infty \tag{9.22}$$

equation (9.19) implies that, to a first approximation,

$$1 - \frac{\rho_0 A_0}{T_1} u = \bar{\eta}_0^{-1}\left(\frac{A_0 t}{D-X}\right)^{-\frac{1}{2}} \quad \text{as} \quad \bar{\eta}_0 \to \infty. \tag{9.23}$$

(i) *Perfectly free interface*

The simplest use of the result (9.10) is to calculate the motion of a perfectly free interface at which $c = 0$ and $A = A_0$. At such an interface equation (9.10) implies that

$$\frac{u}{A_0} = 2\frac{G}{A_0} = -2\frac{F}{A_0} = -2(\mu A_0^{\frac{1}{2}})^{-1} \ln\left[1 - \frac{M}{1-M}\left(\frac{A_0 t}{D} - 1\right)\right]. \tag{9.24}$$

When the incident pulse is described by equations (9.12), equation (9.24) implies that

$$\frac{u}{A_0 e_{\mathrm{I}}} = -\frac{1+M}{M} \ln\left[1 - \frac{M}{1-M}\left(\frac{A_0 t}{D} - 1\right)\right]. \tag{9.25}$$

When the incident pulse is described by equations (9.13) or (9.14), equation (9.24) implies that

$$\frac{\rho_0 A_0}{T_1} u = \tanh^3 \bar{\eta}_0 (\bar{\eta}_0 - \tanh \bar{\eta}_0)^{-1} \ln\left[1 + \cosh^2 \bar{\eta}_0\left(\frac{A_0 t}{D} - 1\right)\right], \tag{9.26}$$

or

$$= \tan^3 \theta_0 (\tan \theta_0 - \theta_0)^{-1} \ln\left[1 + \cos^2 \theta_0\left(\frac{A_0 t}{D} - 1\right)\right]. \tag{9.27}$$

The range of variation of $A_0 t/D$ in equations (9.24) to (9.27) is determined by the range of variations of u in the incident wave. If u varies in the range $[0, u_m]$ in the incident wave, so that G also varies in the range $[0, u_m]$, then equation (9.24) predicts that, at $X = 0$, u varies in the range $[0, 2u_m]$. The value $u = 0$ occurs when $A_0 t/D = 1$, the value $u = 2u_m$ occurs when

$$\frac{A_0 t}{D} = 1 + \frac{1+M}{M}\left(1 - \exp\left[-\mu u_m A_0^{-\frac{1}{2}}\right]\right). \tag{9.28}$$

In the limit as $M \to 1$, when the variation of u in the incident pulse is given by equation (9.15), equation (9.25) predicts that, to a first approximation, the variation of u at the interface is given by

$$\frac{u}{A_0 e_I} = -2\ln\left[1 - \frac{1}{1-M}\left(\frac{A_0 t}{D} - 1\right)\right] \quad (M \to 1). \tag{9.29}$$

Consequently, the time variation of u is logarithmic like in the incident wave: only the amplitude is doubled. In the limit as $M \to 0$, when the variation of u in the incident pulse is described by equation (9.17), equation (9.25) predicts that at the interface

$$\frac{u}{A_0 e_I} = \frac{A_0 t}{D} - 1. \tag{9.30}$$

In the limit as $\bar{\eta}_0 \to 0$, when the variation of u in the incident pulse is described by equation (9.19), equation (9.26) predicts that at the interface

$$\frac{\rho_0 A_0}{T_I} u = 3\ln\left(\frac{A_0 t}{D}\right). \tag{9.31}$$

Finally, in the non-uniform limit as $\bar{\eta}_0 \to \infty$, when the variation of u in the incident pulse is described by equation (9.19), equation (9.26) predicts that

$$\frac{\rho_0 A_0}{T_I} u = \bar{\eta}_0^{-1} \ln\left[1 + \tfrac{1}{4} e^{2\bar{\eta}_0}\left(\frac{A_0 t}{D} - 1\right)\right] \quad \text{as} \quad \bar{\eta}_0 \to \infty. \tag{9.32}$$

Except for the factor 1/2, the variation of u with $A_0 t/D$ described by this equation is identical with that of u with $A_0 t/D - X$, which is given by equation (9.21), at the front of the incident pulse. However, whereas equation (9.21) is only valid near the front of the incident wave where condition (9.20) holds, equation (9.32) is valid for $1 \leqslant A_0 t/D \leqslant 5$. Equation (9.32) still predicts that $\rho_0 A_0 u/T_I$ changes rapidly at the arrival of the front at the interface. Now, however, it can change from zero to any value < 2 rather than from zero to any value < 1 like in the incident pulse. There is one other important difference. Whereas the limiting value of $\rho_0 A_0 u/T_I$ can only be attained asymptotically as $A_0 t/D - X \to \infty$ in the incident pulse (see equation (9.23)), at the interface the limiting value occurs when $A_0 t/D = 5$. This is easily seen by noting that over times where

$$\bar{\eta}_0\left(2 - \frac{\rho_0 A_0}{T_I} u\right) = o(1) \quad \text{as} \quad \bar{\eta}_0 \to \infty, \tag{9.33}$$

equation (9.32) predicts that, to a first approximation,

$$2 - \frac{\rho_0 A_0}{T_I} u = \tfrac{1}{4}\bar{\eta}_0^{-1}\left(5 - \frac{A_0 t}{D}\right). \tag{9.34}$$

In figures 17 and 18 we have compared typical variations of u with $A_0 t/D$ at the interface against their variations with $A_0 t/D - X$ in the incident pulse. The cases $M = 0$ and $\bar{\eta}_0 = 0$ have

been included. The reflexion from a free surface for a gas has also been included. This is of significance when discussing the reflexion of a centred wave from a strong contact discontinuity.

The displacement x of the interface can be calculated by integrating equation (9.24). It is given by

$$\frac{x}{D} = 2(\mu A_0^{\frac{1}{2}})^{-1}\frac{1-M}{M}[(1+t^*)\ln(1+t^*)-t^*], \tag{9.35}$$

where

$$t^* = -\frac{M}{1-M}\left(\frac{A_0 t}{D}-1\right). \tag{9.36}$$

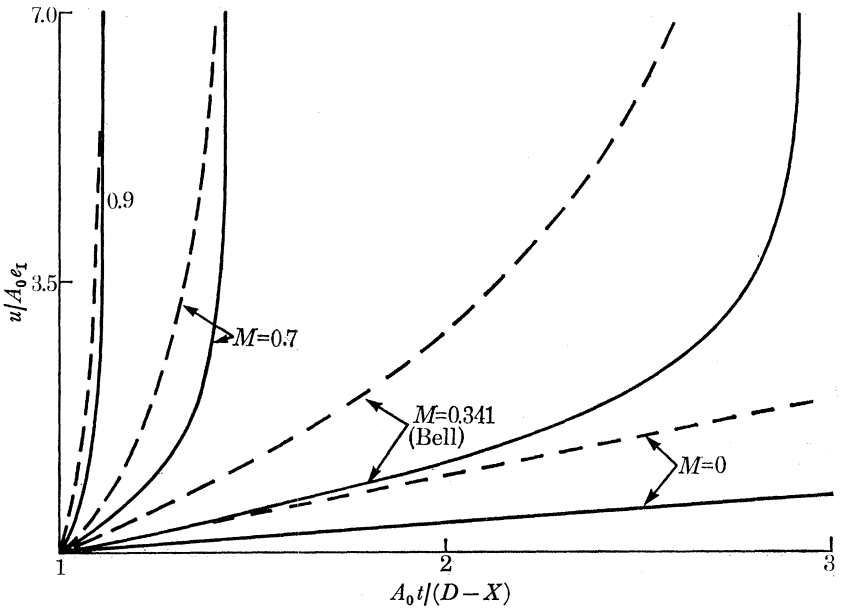

FIGURE 17. u against $A_0 t/(D-X)$ in an incident centred wave (———) and u against $A_0 t/D$ (— —) during its reflexion from a perfectly free interface: non-ideal materials.

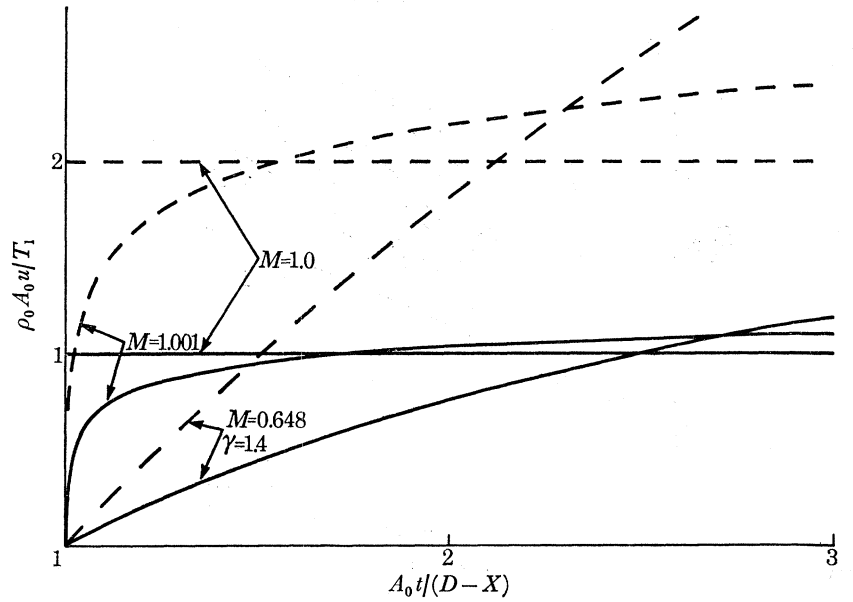

FIGURE 18. u against $A_0 t/(D-X)$ in an incident centred wave (———) and u against $A_0 t/D$ (— —) during its reflexion from a perfectly free interface: ideal materials.

This relation is depicted in figure 19. For non-ideally soft materials $-1 \leqslant t^* \leqslant 0$, for ideally soft materials $t^* \geqslant 0$. In an ideally soft material the amplitude of x/D increases without bound as the amplitude of the incident pulse increases. By contrast, in a non-ideally soft material, no matter how large the amplitude of the incident pulse, x/D has a limiting value of

$$(1-M^2)\,e_{\mathrm{I}}/M^2. \tag{9.37}$$

In practice the centred simple wave only comprises part of the incident pulse. The simplest situation to analyse is when the traction remains constant for some time at $X = D$ after changing discontinuously to produce the centred wave. This occurs in the shock-tube problem, and in a

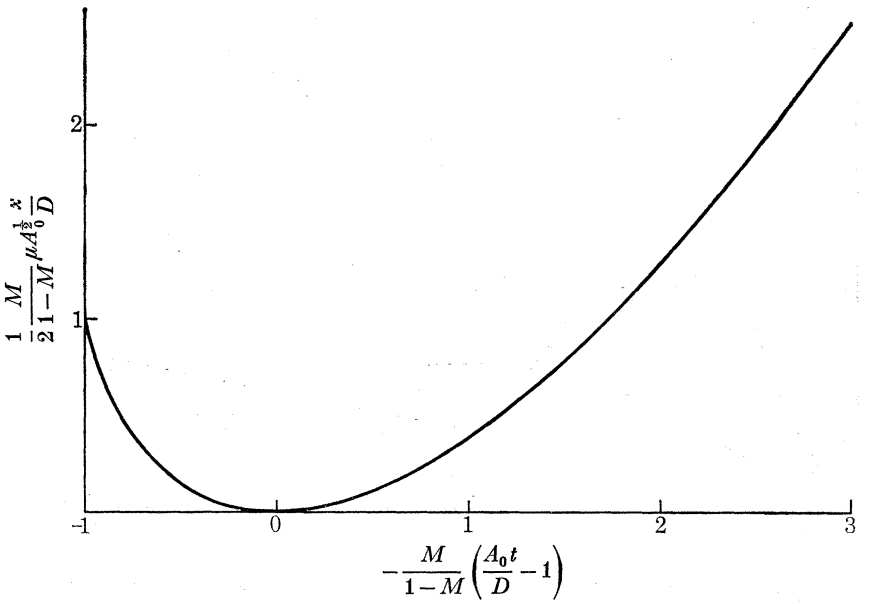

FIGURE 19. The variation of the displacement x of a free interface during the reflexion of a centred simple wave.

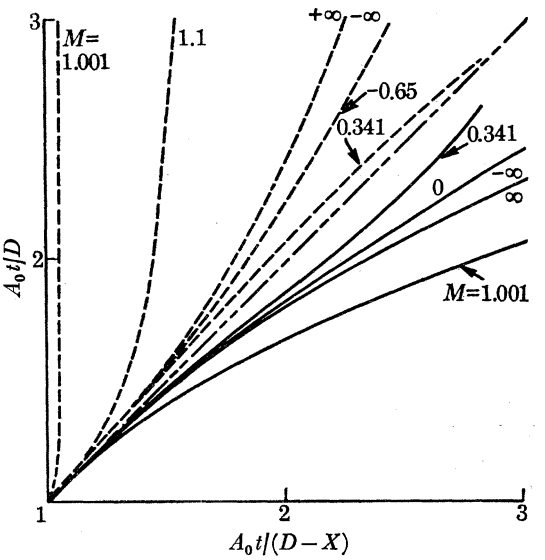

FIGURE 20. The variation in the duration of a pulse at an interface as a function of its duration at any particle X in the incident centred wave. The full curves (———) correspond to a perfectly free boundary at which the duration of the pulse shortens and the broken curves (– – – –) to a perfectly rigid boundary at which the duration lengthens. For a Hookean material ($M = 1$) there is no shortening or lengthening.

string which is suddenly pulled and then held at constant tension. Then, the centred wave takes the material from one uniform state to some other uniform state. In figure 20 we have plotted the time interval which separates these uniform states at the free interface as a function of the time interval which separates them in the incident wave.

(ii) *Perfectly rigid interface*

Another important use of equation (9.10) is to calculate the variation in traction at a rigid interface If

$$\text{at } X = 0, \quad u = 0 \quad \text{then} \quad G = F = \tfrac{1}{2}c \tag{9.38}$$

and equation (9.10) implies that the variation of c with t is given by

$$\frac{A_0 t}{D} = 1 + \frac{1-M}{M}\left(1 - \exp\left[-\tfrac{1}{2}\mu \int_0^c A^{-\frac{1}{2}}\,\mathrm{d}c\right]\right) \tag{9.39}$$

$$= 1 + \frac{1-M}{M}\left(1 - [\cosh \bar{c} + M^{\frac{1}{2}} \sinh \bar{c}]^{-1}\right) \quad \text{when } A \text{ is given by (8.35)}, \tag{9.40}$$

$$= 1 + \operatorname{sech}^2 \bar{\eta}_0 \left(\frac{\sinh \bar{\eta}_0}{\sinh (\bar{\eta}_0 + \bar{c})} - 1\right) \quad \text{when } A \text{ is given by (8.48)}, \tag{9.41}$$

$$= 1 + \sec^2 \theta_0 \left(\frac{\sin \theta_0}{\sin (\theta_0 + \bar{c})} - 1\right) \quad \text{when } A \text{ is given by (8.62)}. \tag{9.42}$$

Once the variation of $\bar{c}$ with t has been calculated from any one of the equations (9.40) to (9.42) the variations of T, e and c with t can be computed from the appropriate equations which are given in §8.3. The variations of G and F with t then follow from equation (9.38). If $\bar{c}$ varies over the range $[0, \bar{c}_\mathrm{m}]$ in the incident wave, then at the rigid interface $\bar{c}$ varies over the range $[0, 2\bar{c}_\mathrm{m}]$.

Since $u \equiv 0$ at the interface it is better to compare the variation of the traction T at the interface with its variation in the incident wave. After some algebra, it can be shown that:

$$\text{as} \quad M \to 1, \qquad \frac{T}{T_\mathrm{I}} = \begin{cases} -\ln\left[1 - \dfrac{1}{1-M}\left(\dfrac{A_0 t}{D - X} - 1\right)\right] & \text{in the incident wave,} \\ -2\ln\left[1 - \dfrac{1}{1-M}\left(\dfrac{A_0 t}{D} - 1\right)\right] & \text{at the interface;} \end{cases} \tag{9.43}$$

$$\text{when} \quad M = 0, \qquad \frac{T}{T_\mathrm{I}} = \begin{cases} 1 - \left(\dfrac{A_0 t}{D - X}\right)^{-\frac{1}{2}} & \text{in the incident wave,} \\ 1 - \left[2\dfrac{A_0 t}{D} - 1\right]^{-\frac{1}{2}} & \text{at the interface;} \end{cases} \tag{9.44}$$

$$\text{when} \quad \bar{\eta}_0 = 0, \qquad \frac{T}{T_\mathrm{I}} = \begin{cases} 1 - \left(\dfrac{A_0 t}{D - X}\right)^{-\frac{3}{2}} & \text{in the incident wave,} \\ 1 - \left(\dfrac{A_0 t}{D}\right)^{-3} & \text{at the interface.} \end{cases} \tag{9.45}$$

As $\bar{\eta}_0 \to \infty$ the variation of T is given implicitly by the relation

$$\frac{A_0 t}{D - X} = \tanh^2 \bar{\eta}_0 \coth^2 (\bar{\eta}_0 [1 - T/T_\mathrm{I}]) \quad \text{in the incident wave,} \tag{9.46}$$

and by

$$\frac{A_0 t}{D} = 1 + \operatorname{sech}^2 \bar{\eta}_0 \left[\frac{\sinh \bar{\eta}_0}{\sinh (\bar{\eta}_0 [1 - T/T_\mathrm{I}])} - 1\right] \quad \text{at the interface.} \tag{9.47}$$

In a layer near the front of the incident pulse where $A_0 t/(D-X) = 1 + O(e^{-2\bar{\eta}_0})$ equation (9.46) predicts that

$$\frac{T}{T_1} = (2\bar{\eta}_0)^{-1} \ln\left[1 + \tfrac{1}{4} e^{2\bar{\eta}_0}\left(\frac{A_0 t}{D-X} - 1\right)\right]. \tag{9.48}$$

At the interface where $A_0 t/D = 1 + O(e^{-2\bar{\eta}_0})$ equation (9.47) predicts that

$$\frac{T}{T_1} = \bar{\eta}_0^{-1} \ln\left[1 + \tfrac{1}{4} e^{2\bar{\eta}_0}\left(\frac{A_0 t}{D} - 1\right)\right]. \tag{9.49}$$

When
$$\bar{\eta}_0[1 - T/T_1] = o(1), \tag{9.50}$$

equations (9.46) and (9.47) predict that

$$1 - \frac{T}{T_1} = \begin{cases} \bar{\eta}_0^{-1}\left(\dfrac{A_0 t}{D-X}\right)^{-\frac{1}{2}} & \text{in the incident wave,} \\ 2\bar{\eta}_0^{-1} e^{-\eta_0}\left(\dfrac{A_0 t}{D} - 1\right)^{-1} & \text{at the interface.} \end{cases} \tag{9.51}$$

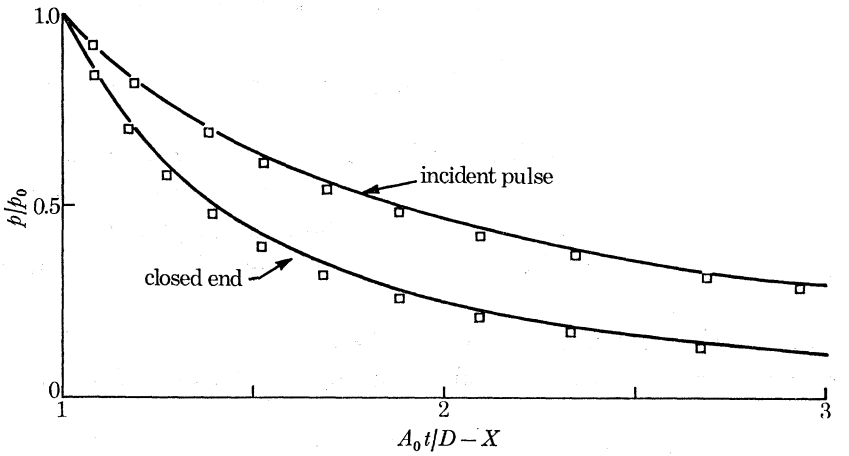

FIGURE 21. The predicted pressure variation at the closed end of a shock tube during the reflexion of a centred simple wave compared with that calculated by Owczarek (1964). ——— Denotes theoretical prediction; □ denote numerical values computed by Owczarek.

In figure 21 we have compared the pressure variation at the closed end of a shock tube which is predicted by the present theory with that computed by Owczarek (1964). According to equations (8.10), (8.13) and (9.42) the theory predicts that the pressure variation on the wall is given parametrically by the relations

$$\frac{p}{p_0} = 1 - \frac{\gamma T}{\rho_0 A_0^2} = -2.4768 + 0.9070\frac{c}{A_0} + 0.2794 \tan\left(0.8921 - 0.03244\frac{c}{A_0}\right) \tag{9.52}$$

and
$$\frac{A_0 t}{D} = 1.9753 \operatorname{cosec}\left(0.8921 - 0.3244\frac{c}{A_0}\right) - 1.5375. \tag{9.53}$$

As can be seen from figure 21 as p varies in the range $p_0 \leqslant p \leqslant 0.1 p_0$ the agreement is remarkably good. The error is of the same order as that in Owczarek's calculations. He used standard graphical techniques.

In figures 22 and 23 the variations of T with $A_0 t/(D-X)$ in the incident centred wave have been compared with their variations with $A_0 t/D$ at a rigid interface. Figure 22 describes the

behaviour of soft materials, figure 23 the behaviour of ideally soft materials. For both classes of materials the stress rate increases at the boundary. For ideally soft materials $T/T_1 < 1$ and the increase in stress rate at the boundaries is very marked. However, as can be seen from figure 20 the total duration of a pulse can lengthen considerably at a rigid interface. The increase in stress rate is due to the increase in stress.

The solution of the rigid interface problem also solves the problem of what happens at the mid-point of an elastic string which softens in extension when the tensions at both ends

$$(X = D \quad \text{and} \quad X = -D)$$

are suddenly increased by the same amount. The centred waves produced at both ends interact near the middle $X = 0$ where $u \equiv 0$.

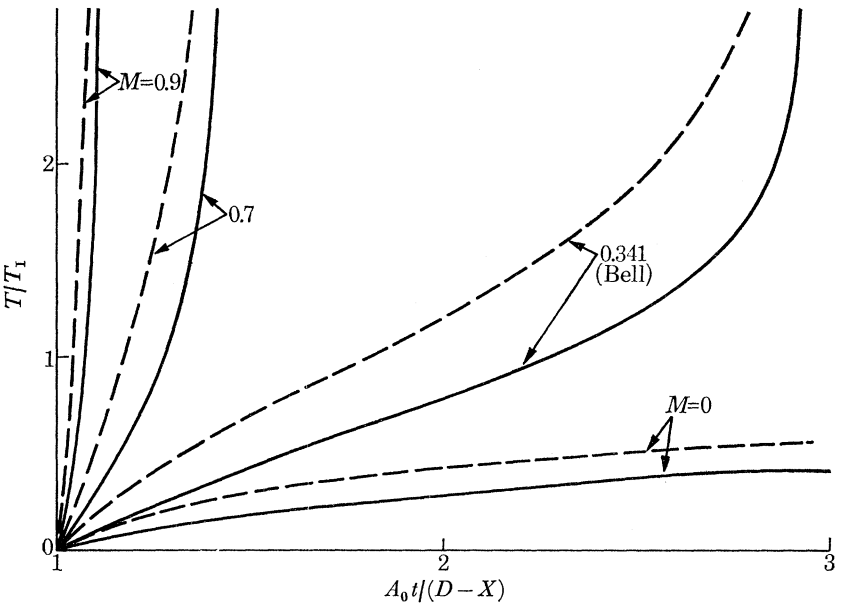

FIGURE 22. T against $A_0t/(D-X)$ in an incident centred wave (———) and T against A_0t/D (— —) during its reflexion from a perfectly rigid interface: non-ideal materials.

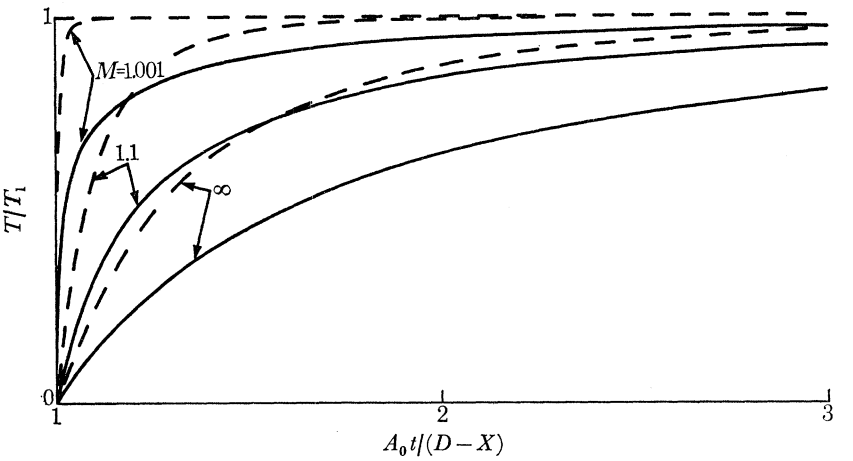

FIGURE 23. T against $A_0t/(D-X)$ in an incident centred wave (———) and T against A_0t/D (— — —) during its reflexion from a perfectly rigid interface: ideal materials.

(iii) *Interface with a Hookean material*

It may happen that the interface $X = 0$ separates two elastic materials which have the property that although the response of the material to the right is grossly nonlinear for the stress level which occurs, the response of that to the left remains essentially linear. As a last application of the result (9.10) we calculate conditions at such an interface during the arrival of a centred simple wave.

In the Hookean material to the left of the interface

$$T_{\mathrm{L}} = \rho_{\mathrm{L}0} A_{\mathrm{L}0} c_{\mathrm{L}}. \tag{9.54}$$

Equations (4.6) and (4.5), which express the continuity of normal traction and material velocity at the interface, then imply that

$$\text{at} \quad X = 0, \quad u = c_{\mathrm{L}} = G_{\mathrm{L}} = \frac{T(c)}{\rho_{\mathrm{L}0} A_{\mathrm{L}0}}, \tag{9.55}$$

so that

$$G = \frac{1}{2}\left[c + \frac{T(c)}{\rho_{\mathrm{L}0} A_{\mathrm{L}0}}\right] \quad \text{and} \quad F = \frac{1}{2}\left[c - \frac{T(c)}{\rho_{\mathrm{L}0} A_{\mathrm{L}0}}\right]. \tag{9.56}$$

According to equations (9.55) and (8.9) at the interface

$$\frac{\mathrm{d}G}{\mathrm{d}c} = \frac{1}{2}\left[1 + i_0^{-1}\frac{A(c)}{A_0}\right] \quad \text{and} \quad \frac{\mathrm{d}F}{\mathrm{d}c} = \frac{1}{2}\left[1 - i_0^{-1}\frac{A(c)}{A_0}\right], \tag{9.57}$$

where

$$i_0 = \frac{\rho_{\mathrm{L}0} A_{\mathrm{L}0}}{\rho_0 A_0} \geqslant 0 \tag{9.58}$$

is the impedance of the interface when the materials on either side are in their reference states. Equations (9.56) define the reflexion function $F = L(G)$ at the interface. The local reflexion coefficient

$$l = \frac{\mathrm{d}F}{\mathrm{d}G} = \frac{i_0 - A/A_0}{i_0 + A/A_0}. \tag{9.59}$$

If the first of equations (9.56) is used to express G in terms of c, equation (9.10) predicts that during the arrival of a centred wave at $X = 0$ the variation of c with t is determined from the condition that

$$\frac{A_0 t}{D} = 1 + \frac{1-M}{M}\left(1 - \exp\left[-\tfrac{1}{2}\mu A_0^{-\frac{1}{2}}\int_0^c \left[\left(\frac{A}{A_0}\right)^{-\frac{1}{2}} + i_0^{-1}\left(\frac{A}{A_0}\right)^{\frac{1}{2}}\right]\mathrm{d}c\right]\right) \tag{9.60}$$

$$= 1 + \frac{1-M}{M}\left(1 - [\cosh\bar{c} + M^{\frac{1}{2}}\sinh\bar{c}]^{-1}[\cosh\bar{c} + M^{-\frac{1}{2}}\sinh\bar{c}]^{-M/i_0}\right)$$

for non-ideally soft materials, (9.61)

$$= 1 + \operatorname{sech}^2\bar{\eta}_0\left[\frac{\sinh\bar{\eta}_0}{\sinh(\bar{\eta}_0 + \bar{c})}\left(\frac{\cosh\bar{\eta}_0}{\cosh(\bar{\eta}_0 + \bar{c})}\right)^{\coth^2\bar{\eta}_0/i_0} - 1\right], \tag{9.62}$$

or

$$= 1 + \sec^2\bar{\theta}_0\left[\frac{\sin\theta_0}{\sin(\theta_0 + \bar{c})}\left(\frac{\cos(\theta_0 + \bar{c})}{\cos\theta_0}\right)^{\cot^2\theta_0/i_0} - 1\right] \tag{9.63}$$

for ideally soft materials. The case of the perfectly rigid interface is obtained from these equations by letting $i_0 \to \infty$. The case of the perfectly free interface is obtained by letting both $i_0 \to 0$ and $\bar{c} \to 0$, while the ratio $c/i_0 (\propto \bar{c}/i_0) \to u$. Once the variation of $\bar{c}$ with t has been determined from

any of the equations (9.61) to (9.63) the corresponding variation of T can be calculated from equation (8.33), or equation (8.46), or equation (8.60). The variation of u then follows from equation (9.55).

According to equations (9.61) and (8.33) in the limit

$$\text{as} \quad M \to 1, \quad \frac{T}{T_1} = -\frac{2i_0}{1+i_0} \ln\left[1 - \frac{1}{1-M}\left(\frac{A_0 t}{D} - 1\right)\right]. \tag{9.64}$$

In the limit as $M \to 0$, T cannot be determined as an explicit function of t but is given by the implicit relation

$$\frac{A_0 t}{D} = \frac{1}{2}\left[1 + \left(1 - \frac{T}{T_1}\right)^{-2} - 2i_0^{-1} \ln\left(1 - \frac{T}{T_1}\right)\right], \quad (M = 0). \tag{9.65}$$

In the limit as $\bar{\eta}_0 \to 0$ equations (9.62) and (8.46) imply that T is related to t by the condition that

$$\frac{A_0 t}{D} = \left(1 - \frac{T}{T_1}\right)^{-\frac{1}{3}} \exp\left[\frac{1}{2i_0}\left(1 - \left[1 - \frac{T}{T_1}\right]^{\frac{2}{3}}\right)\right]. \tag{9.66}$$

The limiting behaviour as $\bar{\eta}_0 \to \infty$ ($M \to 1$ from values > 1) is of special interest (see figure 13). In this limit the first of equations (8.53) and (9.56) imply that

$$\frac{T}{T_1} = \frac{\rho_0 A_0}{T_1} G \quad \text{in the incident pulse} \tag{9.67}$$

while

$$\frac{T}{T_1} = \frac{2i_0}{1+i_0} \frac{\rho_0 A_0}{T_1} G \quad \text{at the interface.} \tag{9.68}$$

These equations imply that if $\sigma (< 1)$ denotes the maximum value of T/T_1 in the centred incident wave then the maximum value of T/T_1 at the interface can never exceed

$$\bar{\sigma} = 2i_0 \sigma / (1 + i_0). \tag{9.69}$$

However, T/T_1 will only attain the value $\bar{\sigma}$ at the interface if the characteristic β-wavelet which carried the stress level $T = \sigma T_1$ in the incident wave reaches it. This is always so when $i_0 < 1$. Then, since $\sigma < 1$, T/T_1 can never exceed the value $2i_0/(1+i_0)$ at the interface. However, when $i_0 > 1$ only those wavelets at which $T/T_1 < (1+i_0)/2i_0$ in the incident wave reach the interface. This is suggested by equations (9.67) and (9.68) and the fact that T/T_1 can never exceed unity. To prove it note that, according to equations (9.46) and (9.62), in that part of the wave

$$\text{where} \quad \bar{\eta}_0 (1 - T/T_1) \to \infty \quad \text{as} \quad \bar{\eta}_0 \to \infty, \tag{9.70}$$

$$\frac{A_0 t}{D - X} = 1 + 4\left[\exp\left\{-2\bar{\eta}_0\left(1 - \frac{T}{T_1}\right)\right\} - \exp\{-2\bar{\eta}_0\}\right] \quad \text{in the incident wave,} \tag{9.71}$$

while

$$\frac{A_0 t}{D} = 1 + 4\left[\exp\left\{-2\bar{\eta}_0\left(1 - \frac{1+i_0}{2i_0}\frac{T}{T_1}\right)\right\} - \exp\{-2\bar{\eta}_0\}\right] \quad \text{at the interface.} \tag{9.72}$$

Equation (9.71) implies that, as $\bar{\eta}_0 \to \infty$, T/T_1 changes discontinuously from 0 to σ in the incident pulse. Equations (9.69), (9.70) and (9.72) imply that, when $i_0 < 1$, T/T_1 changes discontinuously from 0 to $\bar{\sigma}$ at the interface. When $i_0 > 1$ condition (9.73) still implies that T/T_1 cannot exceed $2i_0/(1+i_0)$ However, as T/T_1 approaches unity condition (9.70) is violated so that when $i_0 > 1$

equation (9.72) does not tell the whole story. In fact, T/T_1 cannot exceed unity. This is easily seen by noting that, according to equations (9.46) and (9.62), in that part of the wave

$$\text{where} \quad \bar{\eta}_0(1 - T/T_1) \to 0 \quad \text{as} \quad \bar{\eta}_0 \to \infty, \tag{9.73}$$

$$1 - \frac{T}{T_1} = \begin{cases} \bar{\eta}_0^{-1} \left(\dfrac{A_0 t}{D - X} \right)^{-\frac{1}{2}} & \text{in the incident wave,} \\ \bar{\eta}_0^{-1} \, (\cosh \bar{\eta}_0)^{-(i_0 - 1)/i_0} \left(\dfrac{A_0 t}{D} - 1 \right)^{-1} & \text{at the interface.} \end{cases} \tag{9.74}$$

Consequently, for a large but finite value of $\bar{\eta}_0$, in both the incident wave and at the interface, T can only attain its limiting value T_1 asymptotically as either $A_0 t/(D - X)$, or $A_0 t/D, \to \infty$. Note that T/T_1 will approach unity at the interface whenever $T/T_1 > (1 + i_0)/2i_0$ in the incident wave.

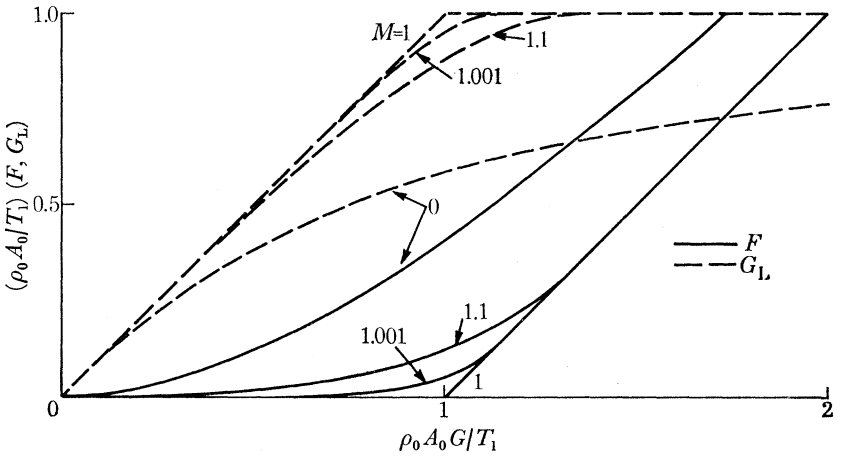

FIGURE 24. The amplitudes, F and G_L, of the reflected and transmitted waves as functions of G, the amplitude of the incident wave, at an interface with a Hookean material. In their reference configurations the impedances of the two materials match ($i_0 = 1$) so that sufficiently small amplitude pulses are not significantly reflected.

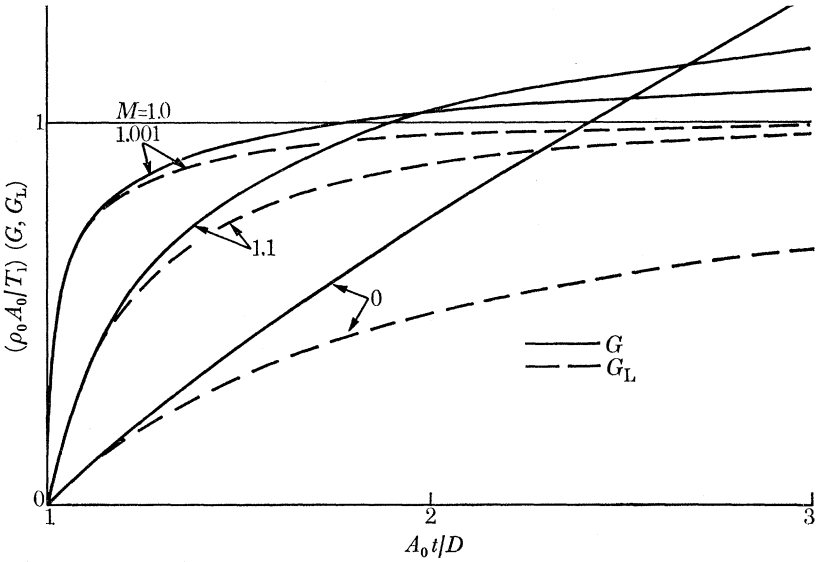

FIGURE 25. Variation of G and G_L with t at the interface with a Hookean material when $i_0 = 1$ during the reflexion and transmission of an incident centred wave.

In figure 24 we have depicted typical variations of F and G_L with G at an interface which separates a model material from a material which satisfies Hooke's law. We have taken $i_0 = 1$ so that the impedances of the two materials match in the reference state and have concentrated on materials for which A/A_0 stays close to unity until T approaches its limiting value T_1 when $A/A_0 \to 0$. This means that the reflexion coefficient l (see equation (9.59)) is essentially zero until T approaches T_1 where it suddenly changes to unity. Consequently, that part of the incident pulse in which $T/T_1 < 1$ is transmitted at the interface without appreciable reflexion while that part in which T approaches its limiting value T_1 is almost completely reflected. The reflexion characteristics of the interface, which are described by equations (9.55) and (9.56), are independent of the shape of the incoming pulse. In figure 25 we show G and G_L vary with t at an interface with the characteristics depicted in figure 24 when the incoming pulse is a centred wave.

The results presented in this paper were obtained in the course of research sponsored by the U.S. Army under contract no. DAAD05-71-C-0389 and monitored by the Ballistics Research Laboratories, Aberdeen Proving Ground, Md.

References

Allen, W. A., Mayfield, E. B. & Morrison, H. L. 1957 *J. appl. Phys.* **28**, 370.
Bell, J. F. 1968 *The physics of large deformations of crystalline solids*. New York: Springer-Verlag.
Cole, R. H. 1948 *Underwater explosions*. Princeton University Press.
Courant, R. & Friedrichs, K. O. 1948 *Supersonic flow and shock waves*. New York: Interscience.
Cristescu, N. 1967 *Dynamic plasticity*. New York: John Wiley and Sons, Inc.
Ginsburg, T. 1964 *J. struct. Div. Am. Soc. civ. Engrs* **90**, no. STI, 125.
Hampton, D. & Huck, P. J. 1968 *Study of wave propagation in confined soils*. Chicago: I.I.T. Research Institute Contract Report S-69-2.
Liahov, G. M. 1964 *The fundaments of the dynamics of explosions in soils*. Moscow.
Mortell, M. P. & Varley, E. 1970 *Proc. R. Soc. Lond.* A **318**, 169.
Owczarek, J. A. 1964 *Fundamentals of gas dynamics*. Scranton: International Textbook Co.
Varley, E. & Cumberbatch, E. 1970 *J. Fluid Mech.* **43**, 513.

PHILOSOPHICAL TRANSACTIONS OF THE ROYAL SOCIETY A MATHEMATICAL, PHYSICAL & ENGINEERING SCIENCES